High-resolution paleoproductivity fluctuations during the past 24 kyr as indicated by benthic foraminifera in the marginal Arctic Ocean[☆]

Jutta E. Wollenburg [a], Jochen Knies [b], Andreas Mackensen [a,*]

[a] *Alfred Wegener Institute for Polar and Marine Research, Columbusstrasse, 27568 Bremerhaven, Germany*
[b] *Geological Survey of Norway, 7491 Trondheim, Norway*

Abstract

Analyses of benthic foraminifera in sediment cores taken at about 1000 m water depth at the Yermak Plateau and the Barents Sea slope, adjacent to the position of the ice-sheet edge during the Last Glacial Maximum, show that paleoproductivity was reduced to about a third of its present level during peak glacial stadials. These reduced values are still higher than values for modern, permanently ice-covered regions, suggesting that the core locations were at least partially ice-free even during stadials. Paleoproductivity at the core locations was higher than or equal to that of today during initial deglaciations and warm substages. Peak paleoproductivity occurred in samples with low-salinity surface waters as indicated by oxygen isotope values of planktonic foraminifera, and slightly after increased abundance of 'Atlantic species', suggesting that enhanced advection of warmer waters from the Atlantic supported the initial ice-sheet retreat. During the Holocene Climatic Optimum productivity was much less than at present on the Yermak Plateau, high at the Barents Sea site, perhaps because of increased advection of Atlantic water to the latter site and heavier ice coverage at the former. After this optimum, paleoproductivity at both sites was similar, with slightly lower values during cold periods such as the Little Ice Age.
© 2003 Elsevier B.V. All rights reserved.

Keywords: foraminifera; productivity; Arctic Ocean; Weichselian; deglaciation

1. Introduction

The Arctic Ocean plays a crucial role in Earth's climate, but is one of its least known oceanic regions. Freshwater transport from the Arctic into the North Atlantic has a strong influence on the global thermohaline circulation (e.g. Sarnthein et al., 2000). This transport can change the southward branch of thermohaline circulation, and trigger a reduction in volume of North Atlantic Deep Water formed, and/or a decrease in depth of this water mass (e.g. Dickson et al., 1988; Oppo and Lehman, 1995; Rahmstorf, 1995; Belkin et al., 1998; Sarnthein et al., 2000). We studied the northward branch of the thermohaline conveyor belt (Fig. 1), which ultimately drives heat into the

Arctic Ocean, and thus influences northern hemispheric climate. In the Eurasian Basin this heat flow affects the time and extent of seasonal sea-ice retreat, and thus oceanic primary productivity. According to CLIMAP, 1981, relatively warm water flow from the Atlantic into the Arctic was interrupted during glacial periods, and a more or less permanent sea-ice cover extended from the northernmost North Atlantic into the Arctic Ocean during Greenland Stadial 2 (GS-2). More recent investigations, however, suggest that such Atlantic waters were advected into the Arctic for sustained intervals during GS-2, which were called Nordway events; during these events sea-surface conditions were seasonally ice-free around shelf-based ice sheets (Hebbeln et al., 1994; Dokken and Hald, 1996; Knies et al., 1999; Hald et al., 2001). The paleoproductivity in the Arctic Ocean and the waxing/waning of the shelf-based ice sheets were probably profoundly influenced by these advective events (Forman et al., 1995; Hebbeln and Wefer, 1997; Kotlyakov et al., 1998; Landvik et al., 1998; Mangerud et al., 1998, 2002; Svendsen et al., 1999; Fig. 1). Major re-
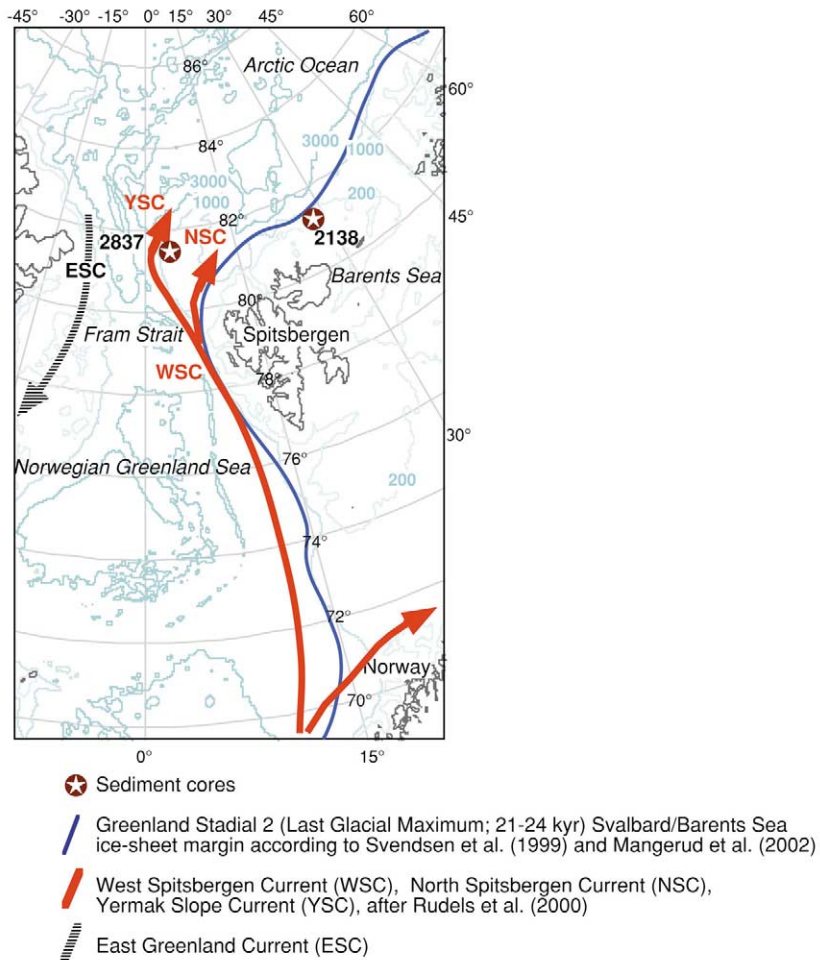

Fig. 1. Overview of the study area showing locations of the investigated sediment cores and surface samples used for transfer function. Also shown is the general circulation pattern in the study area and the GS-2c (LGM) Svalbard–Barents Sea ice-sheet extent.

treats of such ice sheets during the advective events may be reflected in $\delta^{18}O$ meltwater spikes, short intervals with abnormally light oxygen isotope values in planktonic foraminifera, in sediments deposited in the Fram Strait through the central Arctic Ocean between 17.8 and 13.5 ka (e.g. Jones and Keigwin, 1988; Stein et al., 1994; Nørgaard-Pedersen et al., 1998). These Nordway events may correspond to coeval surging events of the Laurentide ice sheet as also recorded in sediment cores from lower latitudes in peaks of ice-rafted debris (IRD) and abnormally light oxygen isotope values in planktonic foraminifera, and be indicative of short-term warming in the Arctic Ocean (e.g. Knies et al., 2000). Environmental conditions analogous to modern ones were established at 10.7–9.1 kyr BP with the final decay of the shelf-based ice sheet (Polyak and Mikhailov, 1996; Hald and Aspeli, 1997; Hald et al., 1999). A warmer period, the Holocene Climate Optimum, is recorded in the Greenland Ice sheets between 8.6 and 4.2 kyr BP (Johnsen et al., 2001).

In most oceanic regions, the concentration of total organic carbon (TOC) in sediments reflects the production of marine organic carbon, and paleoproductivity thus can be estimated from TOC (e.g. Sarnthein et al., 1992). This is not possible in the Arctic Ocean, because significant amounts of refractory, terrestrial organic carbon are released by coastal erosion and transported into the basin by rivers (Reimnitz et al., 1988; Schubert and Stein, 1996; Are, 1999; Fahl and Stein, 1999; Knies et al., 1999, 2000; Stein et al., 1999; Boucsein and Stein, 2000; Boucsein et al., 2000; Stein and Fahl, 2000). Arctic paleoproductivity thus has been estimated qualitatively using organic biomarkers (*n*-alkanes, short-chain fatty acids, and chlorines), ostracods, coccoliths and dinoflagellates (Gard, 1993; Cronin et al., 1994, 1995; Stein et al., 1999; Matthiessen et al., 2001). In contrast, paleoproductivity estimates in subarctic areas are often based on the accumulation rates of calcareous planktonic and benthic foraminifera, suggesting that high accumulation rates reflect high paleoproductivities (e.g. Dokken and Hald, 1996; Nees, 1997; Nees et al., 1997; Struck, 1997; Hald et al., 1999, 2001; Nørgaard-Pedersen et al.,

2003). In accordance, it has been argued from studies of recent Arctic benthic and planktonic foraminifera that their standing stocks (number of living specimens in a standard sample volume) are correlated positively with the marine organic carbon flux (Carstens and Wefer, 1992; Wollenburg and Kuhnt, 2000). In thanatocoenoses, however, this correlation may be lost because carbonate tests suffer intensive dissolution in regions with high organic carbon accumulation rates (Steinsund and Hald, 1994; Hald and Steinsund, 1996; Wollenburg and Kuhnt, 2000). Not only the number of benthic foraminiferal specimens, however, but also the species composition of the assemblages reflects water depth, water-depth-related carbon flux, and the physicochemical character of waters bathing the ocean floor (Green, 1960; Vilks, 1969, 1989; Scott et al., 1989; Scott and Vilks, 1991; Polyak, 1990; Bergsten, 1994; Polyak and Solheim, 1994; Ishman and Foley, 1996; Wollenburg and Mackensen, 1998a; Osterman et al., 1999); these water masses are stratified in the Arctic Ocean.

Loubere (1994) first developed a transfer function to estimate paleoproductivity from relative abundance data of benthic foraminiferal species (e.g. Loubere and Fariduddin, 1999; Loubere, 2000). This method was applied to the Nordic Seas by Kuhnt in Weinelt et al. (2000), to the Arctic Ocean by Wollenburg and Kuhnt (2000) and Wollenburg et al. (2001), although adapted to the high seasonality of productivity in high northern latitudes. Due to the high seasonality of productivity and variable water depths of samples these analyses differ in the statistical method used, correspondence instead of factor analysis, and by using carbon fluxes instead of primary production values for comparison, from those of Loubere and colleagues. In this study we document the paleoproductivity at two sites at approximately 1000 m water depth off the Yermak Plateau (core PS2837) and the Barents Sea slope (core PS2138), adjacent to the position of the Svalbard–Barents Sea ice sheet during the Last Glacial Maximum (LGM; GS-2c) (Fig. 1). Sediments in core PS2837 have a high accumulation rate and thus allowed a high-resolution study of paleoproductivity fluctuation over the last 24 kyr.

Table 1
AMS radiocarbon ages from the investigated cores (Matthiessen et al., 2001; Nørgaard-Pedersen et al., 2003)

Core number	Depth (cm bsf)	^{14}C age (yr BP)	Cal. age (yr BP)	Carbon source	Sample code	Source
PS2138-1	65	$12\,990 \pm 70$	15.52	*N. pachyderma* sin.	KIA9872	1
PS2138-1	110	$13\,590 \pm 80$	16.21	*N. pachyderma* sin.	KIA4765	1
PS2138-1	130	$15\,410 \pm 130$	18.30	*N. pachyderma* sin.	KIA1283	1
PS2138-1	160	$16\,230 \pm 210$	19.24	*N. pachyderma* sin.	KIA364	1
PS2138-1	200	$16\,880 \pm 130$	19.99	*N. pachyderma* sin.	KIA2745	1
PS2138-1	230	$18\,790 \pm 140$	22.19	*N. pachyderma* sin.	KIA9873	1
PS2138-1	244	$19\,270 \pm 130$	22.74	*N. pachyderma* sin.	KIA9874	1
PS2138-1	260	$19\,980 \pm 130$	23.56	*N. pachyderma* sin.	KIA9875	1
PS2138-1	275	$20\,260 \pm 130$	23.88	*N. pachyderma* sin.	KIA9876	1
PS2837-5	10	535 ± 25	194.00	*N. pachyderma* sin.	KIA7570	2
PS2837-5	50	$2\,130 \pm 40$	1723.00	*N. pachyderma* sin.	KIA4652	2
PS2837-5	76	$3\,340 \pm 35$	3\,198.00	*N. pachyderma* sin.	KIA8927	2
PS2837-5	111	$4\,965 \pm 45$	5\,299.00	*N. pachyderma* sin.	KIA8928	2
PS2837-5	153	$7\,405 \pm 45$	7\,864.00	*N. pachyderma* sin.	KIA8929	2
PS2837-5	182	$8\,070 \pm 60$	8\,510.00	*N. pachyderma* sin.	KIA4653	2
PS2837-5	225	$9\,290 \pm 60$	9\,976.00	*N. pachyderma* sin.	KIA8930	2
PS2837-5	253	$10\,940 \pm 50$	12\,470.00	*N. pachyderma* sin.	KIA7571	2
PS2837-5	272–276	$12\,155 \pm 60$	13\,688.00	*N. pachyderma* sin.	KIA10863	2
PS2837-5	300	$12\,655 \pm 60$	14\,195.00	*N. pachyderma* sin.	KIA7572	2
PS2837-5	357–361	$12\,940 \pm 70$	14\,758.00	*N. pachyderma* sin.	KIA10864	2
PS2837-5	382	$16\,040 \pm 80$	16\,629.00	*N. pachyderma* sin.	KIA10865	2
PS2837-5	389	$17\,440 \pm 110$	20\,172.00	*N. pachyderma* sin.	KIA4654	2

All dates were corrected by 440 years for the reservoir effect. Conversion to calibrated years was made using the CALIB 4.3 (Stuiver and Reimer, 1993) program with the data set from Stuiver et al. (1998). Age determinations were carried out at the Leibniz Labor für Altersbestimmung und Isotopenforschung at Kiel University, Germany.

1.1. Modern settings

Temperate, saline Atlantic water enters the Arctic Ocean through the eastern side of Fram Strait (West Spitsbergen Current, WSC) (Fig. 1). On entering the Arctic Ocean, the WSC separates into two branches. The main inflow follows the Svalbard continental slope eastward (North Spitsbergen Current, NSC), while a second, narrower branch stays west and north of the Yermak Plateau (Yermak Slope Current) (Schlichtholz and Houssais, 1999; Rudels et al., 2000). Sea ice, low-salinity surface water, and deeper water masses leave the Arctic Ocean through the western part of the Fram Strait (East Greenland Current).

Arctic primary production is primarily determined by insolation and sea-ice cover. During summer, the warm WSC supports the seasonal ice retreat off Spitsbergen and along the northwestern Barents Sea slope and thus enhances pri-

mary production and benthic life (e.g. Smith et al., 1987; Hibler, 1989; Grebmeier et al., 1995; Piepenburg et al., 1996; Clough et al., 1997; Boetius and Damm, 1998). In the Arctic Ocean data collected by satellites are scarce, confined to seasonally ice-free waters and indicate five to ten times higher primary production values than corresponding conventional ship data (Koblents-Mishke et al., 1968, 1970; Longhurst et al., 1995; Antoine et al., 1996). Until more reliable satellite data become available our estimates of primary production in the Arctic Ocean are based on published 'conventional' data. Such estimates range from 10 to 19 g C m^{-2} yr^{-1} for the permanently ice-covered areas, and from 31 to 59 g C m^{-2} yr^{-1} for continental shelves and slopes of the study area (e.g. English, 1961; Strömberg, 1989; Wassman and Slagstad, 1991; Cota et al., 1991, 1996; Hulth et al., 1994, 1996; Boetius et al., 1996; Wheeler et al., 1996; Gosselin et al., 1997; Melnikov, 1997; Pomeroy, 1997; Zheng et

al., 1998; Louanchi and Najjar, 2001; Appendix Table 1[1]).

2. Material and methods

Kastenlot core PS2837-5 is taken from 1023 m water depth at the Yermak Plateau (81°14′N, 2°23′E) (Stein and Fahl, 1997) (Fig. 1). Because the upper centimeters of the core were disturbed, samples of box core PS2837-6 (1028 m water depth; 81°14′N, 2°25′E) were used to document the upper 21 cm of the sedimentary record. We show data on the upper 4.14 m of the 8.76 m long core. Samples are taken at 1-cm intervals for the upper 50 cm, and 2-cm intervals for the core section down to 100 cm. Below 100 cm samples are taken at intervals of 1–4 cm. A 1-cm sample spacing is used across terminations between stadials and interstadials. According to the stratigraphic model (Nørgaard-Pedersen et al., 2003), the average time resolution is 120 yr per sampling interval. Gravity core PS2138-1 is taken from 995 m water depth off the Barents Sea continental slope (81°32.1′N, 30°35.6′E) (Rachor, 1992). We show data on the upper 2.75 m of the 6.29 m long core. Samples are taken at 2–10-cm intervals, equal to a mean sampling interval of 450 yr. Samples are 1 cm thick, mean sample volume is 24 cm^3, and mean dry weight is 34, 34, and 16 g, for cores PS2837-5, PS2837-6 and PS2138-1, respectively. Where possible, at least 300 specimens are counted from the size fraction > 63 μm (Appendix Tables 2 and 3). The age models are based on 11 (PS2837) and nine (PS2138) accelerator mass spectrometry (AMS) ^{14}C dates, oxygen isotopes and, for the carbonate-poor Holocene core section of PS2138, on dinoflagellates (Tables 1–3; Matthiessen et al., 2001; Nørgaard-Pedersen et al., 2003). This study uses the event stratigraphy based on the δ^{18}O isotopic record of the GRIP Greenland ice-core (INTIMATE[2] group; Björck et al., 1998).

Usually, the water content of Arctic Ocean sediments drops to approximately one third of the surface centimeter within the first 3–5 cm downcore (personal observation). Therefore we decided against core BFAR (foraminiferal counts per 10 cm^3), but instead we calculated weight benthic foraminiferal accumulation rates (WBFAR) from the number of individuals per 10 g dry sediment using mass accumulation rates (MAR) of Knies et al. (1999) and Nørgaard-Pedersen et al. (2003). These MAR are calculated from wet bulk density, porosity and linear interpolated sedimentation rates between stratigraphic tie points using the equation of van Andel et al. (1975). WBFAR is defined as number of specimens per 10 g per kyr.

Estimated carbon flux is calculated from published primary production data (Appendix Table 1) using the equation of Betzer et al. (1984).

For correspondence analysis we used the software package CANOCO 4 (ter Braak and Smilauer, 1998). Core samples containing less than 40 specimens are omitted from correspondence analyses (Tables 2 and 3). The core top sample WBFAR of each site is compared to the modern surface sample BFAR (dead foraminiferal counts per 10 cm^3 of surface sediments; Wollenburg and Kuhnt, 2000 and Appendix Table 4). This correction factor is applied to all WBFAR of each core. Because of the common 'skewed' Gaussian response of benthic organisms to environmental parameters (Jongman et al., 1995), BFAR and corrected WBFAR are transformed by simple logarithmic scaling. In the correspondence analysis the BFAR of 63 surface samples[3] (Wollenburg and Kuhnt, 2000 and Appendix Table 4) are treated as active elements, which define the correspondence analysis factor (CAF). Corrected core

---

[1]   Appendix tables are available electronically on the Elsevier web page and via http://www.pangaea.de/home/jwollenburg.

[2]   INTIMATE: INTegration of Ice-core, MArine and TErrestrial records is a core program of the INQUA (International Quaternary Union) Paleoclimate Commission. The aim is to synthesize data from the marine terrestrial and ice-core realms for the North Atlantic region during the course of the Last Termination.

[3]   The large Laptev Sea data set of Wollenburg and Kuhnt (2000) was omitted to increase the significance of samples under the Atlantic water inflow.

Table 2
Core 2837: core depth, age (kyr BP), correspondence analysis factor 1 value, calculated carbon flux, calculated paleoproductivity, 'phytodetritus species' (%), 'Atlantic species' (%), *Melonis zaandami* (%), *Fontbotia wuellerstorfi* and *Lobatula lobatula* (%), agglutinated foraminifera (%), benthic foraminifera accumulation rate (No. spec. 10 g^{-1} kyr^{-1}), number of specimens counted

Depth (cm bsf)	Cal. age BP (kyr)[+]	CAF1	Cflux (g m^{-2} yr^{-1})	Paleoproductivity (g m^{-2} yr^{-1})	Phytodetritus spec. (%)	Atl.spec. (%)	Melonis zaandami (%)	Cassidulina teretis (%)	Lobatula lobatula and Fontbotia wuellerstorfi (%)	Agglutinated foraminifera (%)	WBFAR (No. spec. 10 g dry sediment^{-1} × Acc. rate kyr^{-1})	No. counted
0	0.00	1.02	1	47	[a]	1	1	6	[a]	72	033 187	453
2	0.04	1.30	2	58	2	[a]	8	5	[a]	72	32 147	363
3	0.06	1.15	1	52	3	[a]	12	3	[a]	68	18 187	427
4	0.08	1.10	1	50	1	[a]	8	[a]	1	79	17 230	316
5	0.10	1.50	2	68	1	1	7	[a]	–	84	18 111	536
6	0.12	1.47	2	67	2	[a]	5	[a]	–	87	11 447	350
7	0.14	1.29	2	58	8	[a]	5	2	[a]	70	7 420	303
8	0.16	1.32	2	59	4	2	11	9	2	38	2 855	235
9	0.17	1.02	1	47	5	4	12	19	2	17	20 039	314
10	0.19	0.91	1	43	6	2	6	17	4	24	24 117	388
11	0.23	0.99	1	45	6	2	7	24	2	23	9 504	326
12	0.27	1.13	1	51	3	1	6	14	[a]	30	7 739	380
13	0.31	1.33	2	60	4	2	12	7	2	46	4 676	306
14	0.35	1.16	1	52	2	[a]	10	10	[a]	33	5 073	369
15	0.39	1.19	1	53	3	2	5	12	[a]	29	7 766	413
16	0.42	1.27	2	57	4	3	8	14	2	42	2 724	171
17	0.46	1.20	1	54	4	1	8	10	[a]	21	5 582	350
18	0.50	1.22	1	55	3	1	8	19	[a]	19	12 948	437
19	0.54	1.22	1	55	2	[a]	12	13	[a]	23	8 337	362
20	0.58	1.10	1	50	2	[a]	10	17	1	20	10 777	354
21	0.61	1.10	1	50	2	1	12	16	2	23	7 149	372
22	0.65	1.21	1	54	3	2	7	26	1	14	1 559	953
23	0.69	1.10	1	50	4	1	6	20	3	18	7 965	416
24	0.73	1.05	1	47	8	2	8	8	1	27	7 616	273
25	0.77	0.98	1	45	8	4	24	12	[a]	15	7 464	332
26	0.81	1.36	2	61	7	4	35	4	1	23	6 865	411
27	0.84	0.92	1	43	3	3	21	14	2	18	11 877	343
28	0.88	1.10	1	50	4	1	16	11	1	33	5 490	364
29	0.92	1.26	2	57	5	2	25	8	[a]	31	4 474	431
30	0.96	1.25	2	56	4	3	12	7	3	36	4 419	416
31	1.00	0.99	1	45	2	2	11	11	2	34	3 248	144

Table 2 (*Continued*).

Depth (cm bsf)	Cal. age BP (kyr)[+]	CAF1	Cflux (g m^{-2} yr^{-1})	Paleoproductivity (g m^{-2} yr^{-1})	Phytodetritus spec. (%)	Atl.spec. (%)	*Melonis zaandami* (%)	*Cassidulina teretis* (%)	*Lobatulalobatula* and *Fontbotiawuellerstorfi* (%)	Agglutinatedforaminifera (%)	WBFAR (No. spec. 10 g dry sediment^{-1} × Acc. rate kyr^{-1})	No. counted
32	1.03	0.87	1	41	2	2	9	16	2	21	9 705	338
33	1.07	1.04	1	47	3	1	14	11	2	36	3 873	141
34	1.11	1.18	1	53	6	2	18	11	1	26	3 238	236
35	1.15	1.31	2	59	1	–	10	14	1	29	656	44
36	1.19	1.25	2	56	4	1	12	10	1	27	2 604	327
37	1.23	1.11	1	50	5	2	6	13	3	24	841	327
38	1.26	0.87	1	41	3	2	8	25	3	16	8 754	661
39	1.30	1.11	1	50	5	2	10	16	[a]	16	7 208	381
40	1.34	0.72	1	36	6	1	8	18	2	20	14 566	337
41	1.38	0.69	1	36	3	2	4	19	1	14	18 037	439
42	1.42	0.85	1	40	3	2	6	24	1	12	10 341	472
43	1.46	0.67	1	35	2	1	4	22	1	17	52 798	299
44	1.49	1.15	1	51	3	2	5	13	1	26	96 789	348
45	1.53	0.84	1	40	3	2	12	22	3	16	12 374	396
46	1.57	0.78	1	38	5	1	5	26	[a]	10	13 521	505
47	1.61	0.70	1	36	4	2	4	20	1	14	17 375	390
48	1.65	1.04	1	47	6	1	16	11	1	29	10 875	348
49	1.68	0.81	1	39	2	–	12	19	2	22	3 988	329
50	1.72	0.60	1	33	3	1	9	16	2	23	15 986	507
52	1.84	0.89	1	42	9	2	26	18	2	6	6 176	323
54	1.95	1.24	2	56	6	2	27	13	1	19	4 245	426
56	2.06	1.21	1	54	2	[a]	19	34	1	18	2 546	315
58	2.18	1.17	1	52	3	2	28	24	1	12	7 363	479
60	2.29	1.21	1	54	1	[a]	23	18	2	19	5 156	364
62	2.40	0.79	1	38	2	[a]	10	35	1	9	7 968	424
63	2.46	1.05	1	47	3	2	24	21	1	20	3 753	353
64	2.52	0.98	1	45	4	4	32	15	2	11	3 525	274
66	2.63	1.21	1	54	3	[a]	21	30	3	11	7 171	508
68	2.74	0.98	1	45	2	[a]	26	23	4	12	1 572	300
70	2.86	1.36	2	61	3	2	21	12	2	29	2 197	317
72	2.97	1.15	1	52	2	[a]	22	16	–	33	1 456	204
74	3.08	1.09	1	49	2	[a]	30	21	8	11	2 166	318
76	3.20	1.02	1	47	3	[a]	28	16	[a]	26	1 890	333
78	3.32	1.21	1	54	3	–	25	11	2	23	2 854	320
80	3.44	1.38	2	62	3	[a]	24	12	2	16	1 464	257

Table 2 (Continued).

Depth (cm bsf)	Cal. age BP (kyr)[+]	CAF1	Cflux (g m^{-2} yr^{-1})	Paleoproductivity (g m^{-2} yr^{-1})	Phytodetritus spec. (%)	Atl.spec. (%)	Melonis zaandami (%)	Cassidulina teretis (%)	Lobatulalobatula and Fontbotiawuellerstorfi (%)	Agglutinatedforaminifera (%)	WBFAR (No. spec. 10 g dry sediment^{-1} × Acc. rate kyr^{-1})	No. counted
82	3.56	1.34	2	60	2	1	21	14	3	19	3 879	383
84	3.68	1.11	1	50	1	3	13	21	1	16	3 128	296
86	3.80	1.30	2	58	1	a	17	11	1	15	5 021	352
88	3.92	0.93	1	43	2	a	11	21	4	8	14 598	317
90	4.04	1.12	1	51	a	a	4	76	a	4	22 690	948
91	4.10	0.79	1	39	2	a	19	19	1	19	5 222	323
92	4.16	0.92	1	43	a	1	10	28	a	7	9 676	440
94	4.28	1.30	2	58	a	1	8	20	1	31	2 144	270
96	4.40	1.50	2	69	–	a	32	4	3	41	626	130
98	4.52	1.73	3	83	a	–	31	3	2	41	2 138	336
99	4.58	1.44	2	65	8	a	31	9	3	26	2 715	279
100	4.64	1.04	1	47	4	–	17	22	5	14	7 664	357
102	4.76	1.48	2	68	6	–	18	23	2	24	2 032	264
106	5.00	1.33	2	60	4	–	23	19	1	27	341	73
108	5.12	1.39	2	63	2	a	11	16	a	5	3 085	452
110	5.24	1.22	1	55	3	–	17	22	2	20	1 995	344
114	5.48	0.75	1	37	a	–	13	12	5	16	8 618	428
118	5.73	1.16	1	52	2	a	36	7	4	23	1 984	306
122	5.97	0.89	1	42	3	–	28	24	5	15	2 094	323
124	6.09	0.91	1	42	a	–	40	12	5	20	1 703	306
126	6.22	1.01	1	46	a	–	27	14	8	11	2 283	295
128	6.34	0.87	1	41	2	a	46	4	1	14	1 378	241
130	6.46	0.92	1	43	a	a	11	18	5	11	3 621	357
132	6.58	0.73	1	37	1	a	11	15	1	7	2 538	279
134	6.70	0.67	1	35	5	a	37	11	6	8	1 819	307
138	6.95	0.69	1	35	5	a	35	8	4	9	3 854	343
142	7.19	0.93	1	43	a	–	76	a	4	7	2 588	340
146	7.44	0.37	1	27	–	–	46	10	8	4	7 788	353
150	7.68	0.77	1	38	a	–	24	8	3	5	13 204	421
154	7.89	0.56	1	32	a	a	27	14	2	4	31 957	393
158	7.98	0.62	1	33	1	–	23	8	5	5	20 163	356
162	8.06	0.51	1	31	a	–	47	6	2	6	6 703	348
165	8.13	0.54	1	31	1	–	31	5	a	5	9 342	272
166	8.15	1.14	1	51	2	–	61	2	4	9	4 389	239
170	8.24	0.53	1	31	1	2	26	20	5	3	17 931	515

Table 2 (*Continued*).

Depth (cm bsf)	Cal. age BP (kyr)[+]	CAF1	Cflux (g m^{-2} yr^{-1})	Paleoproductivity (g m^{-2} yr^{-1})	Phytodetritus spec. (%)	Atl.spec. (%)	Melonis zaandami (%)	Cassidulina teretis (%)	Lobatula lobatula and Fontbotia wuellerstorfi (%)	Agglutinated foraminifera (%)	WBFAR (No. spec. 10 g dry sediment^{-1} × Acc. rate kyr^{-1})	No. counted
174	8.33	0.65	1	34	–	2	46	6	6	4	10 973	411
178	8.42	0.45	1	29	a	a	29	5	5	4	18 842	460
182	8.51	0.60	1	33	a	2	14	5	7	2	39 737	545
186	8.65	0.51	1	31	1	3	11	4	a	6	40 067	402
190	8.78	0.72	1	36	–	1	38	3	4	8	14 285	374
194	8.92	0.50	1	30	1	2	17	5	3	4	29 133	463
198	9.06	0.46	1	29	2	2	14	5	3	3	74 535	391
202	9.19	0.74	1	37	a	1	47	11	3	7	9 619	464
206	9.33	0.80	1	39	–	a	56	6	3	8	5 794	456
210	9.46	0.66	1	34	a	1	32	8	2	8	10 043	449
214	9.60	0.72	1	36	a	a	33	5	1	12	14 823	455
218	9.74	0.76	1	37	1	3	25	6	4	16	7 252	436
222	9.87	0.56	1	32	a	a	22	11	5	8	11 355	494
226	10.07	0.93	1	43	a	a	21	6	1	13	5 102	408
228	10.24	0.62	1	33	a	–	24	3	a	10	3 545	575
230	10.42	1.68	2	78	2	a	29	2	1	39	1 036	323
232	10.60	1.44	2	64	3	–	22	2	2	28	1 984	358
234	10.78	1.57	2	71	a	–	22	11	a	19	1 688	316
237	11.04	1.44	2	64	a	–	4	13	a	5	2 621	341
238	11.13	1.56	2	71	1	a	10	13	a	16	6 322	389
240	11.22	1.24	1	55	a	–	14	15	a	17	283	300
241	11.40	1.33	2	59	5	1	3	16	a	15	5 462	327
242	11.49	1.40	2	62	2	a	13	12	a	11	3 593	443
243	11.58	1.11	1	49	2	–	24	31	a	4	2 944	317
244	11.67	1.15	1	51	2	a	16	31	1	5	1 715	254
246	11.85	1.15	1	51	a	a	8	56	1	4	3 205	393
248	12.02	1.15	1	51	2	1	19	19	–	4	1 605	275
250	12.20	0.98	1	44	a	a	6	42	1	3	12 921	502
251	12.29	0.86	1	40	a	a	5	27	a	8	8 502	323
252	12.38	0.79	1	38	1	1	6	24	–	11	16 064	391
254	12.52	0.77	1	37	1	2	10	19	1	4	17 345	520
258	12.73	0.67	1	34	1	3	16	18	1	2	23 297	396
260	12.83	0.65	1	34	–	–	–	8	–	a	5 804	266
262	12.94	–	–	–	–	–	–	–	–	–	–	–
264	13.05	–	–	–	–	–	–	–	–	–	–	–

Table 2 (*Continued*).

Depth (cm bsf)	Cal. age BP (kyr)[+]	CAF1	Cflux (g m^{-2} yr^{-1})	Paleoproductivity (g m^{-2} yr^{-1})	Phytodetritus spec. (%)	Atl.spec. (%)	*Melonis zaandami* (%)	*Cassidulina teretis* (%)	*Lobatulalobatula* and *Fontbotiawuellerstorfi* (%)	Agglutinatedforaminifera (%)	WBFAR (No. spec. 10 g dry sediment^{-1} × Acc. rate kyr^{-1})	No. counted
265	13.11	–	–	–	–	–	–	–	–	100	7	2
266	13.17	–	–	–	–	–	–	–	–	100	38	5
268	13.30	–	–	–	–	–	–	–	–	67	12	3
270	13.43	1.65	2	75	–	–	15	–	–	85	272	49
272	13.56	1.54	2	69	a	a	84	1	2	4	2 806	339
274	13.69	1.21	1	53	2	–	59	14	3	1	7 127	372
278	13.77	1.02	1	45	a	–	30	53	a	2	142 465	528
282	13.84	1.33	2	58	a	–	35	49	a	5	45 688	395
286	13.92	1.23	1	54	a	–	22	62	a	4	110 601	510
290	14.00	1.18	1	51	a	–	44	44	3	3	88 905	436
294	14.08	1.31	2	57	1	–	22	67	1	3	215 217	474
298	14.16	1.20	1	52	a	a	4	87	a	3	321 618	428
302	14.21	1.30	2	56	a	–	13	71	a	10	371 153	380
306	14.25	1.70	3	78	–	–	25	51	1	21	3 106	83
310	14.29	1.34	2	58	a	–	9	77	a	7	141 612	414
312	14.31	1.61	2	72	2	–	5	82	a	8	201 261	410
313	14.32	1.62	2	73	a	–	6	72	–	13	173 871	492
314	14.33	1.74	3	80	a	–	3	66	a	20	161 731	399
316	14.35	1.75	3	81	a	–	3	57	a	29	135 275	403
318	14.37	1.73	3	80	–	–	1	78	–	15	123 009	399
322	14.40	1.25	2	54	a	–	a	87	a	3	58 476	416
326	14.44	0.91	1	41	a	–	a	72	–	–	28 189	469
330	14.48	0.42	1	28	a	–	–	25	–	–	81 526	433
334	14.52	0.74	1	35	a	–	–	28	–	–	71 848	481
338	14.56	1.05	1	46	a	–	a	13	–	1	34 478	415
342	14.60	1.11	1	48	a	–	a	10	–	3	53 493	489
346	14.63	1.05	1	46	a	–	2	34	–	3	31 823	407
350	14.67	1.06	1	46	2	–	1	66	a	a	103 086	449
354	14.71	1.48	2	64	3	–	1	54	–	9	80 327	448
358	14.75	1.51	2	66	3	–	5	57	1	13	98 220	437
362	14.88	1.48	2	64	1	–	12	62	–	6	24 163	453
366	15.05	1.27	2	54	a	–	4	66	a	2	74 341	461
370	15.21	1.47	2	63	a	–	10	58	a	4	41 226	404
374	15.69	1.16	1	49	a	–	7	41	a	4	20 476	594
376	15.94	1.20	1	51	–	–	16	30	a	3	15 784	342

Table 2 (*Continued*).

Depth (cm bsf)	Cal. age BP (kyr)[+]	CAF1	Cflux (g m^{-2} yr^{-1})	Paleoproductivity (g m^{-2} yr^{-1})	Phytodetritus spec. (%)	Atl.spec. (%)	*Melonis zaandami* (%)	*Cassidulina teretis* (%)	*Lobatula lobatula* and *Fontbotia wuellerstorfi* (%)	Agglutinated foraminifera (%)	WBFAR (No. spec. 10 g dry sediment^{-1} × Acc. rate kyr^{-1})	No. counted
378	16.17	1.17	1	49	a	–	21	20	a	8	18 760	492
382	16.63	0.59	1	31	1	4	4	55	a	2	87 045	1382
383	17.14	0.81	1	37	a	6	6	57	a	3	14 453	427
384	17.64	0.54	1	30	4	8	a	67	1	4	44 061	332
385	18.15	0.26	0	24	5	6	2	63	a	3	42 856	474
386	18.65	0.48	1	28	3	4	a	66	1	2	41 091	100
387	19.16	0.29	1	24	2	5	–	58	a	2	56 238	293
388	19.67	−0.08	0	18	2	7	a	63	a	6	52 527	436
389	20.17	0.20	0	23	a	a	a	82	a	a	27 600	437
390	20.69	0.17	0	22	–	–	1	81	a	–	61 160	419
391	21.20	0.07	0	20	–	–	2	72	–	–	83 113	433
392	21.50	0.02	0	20	a	–	–	72	–	–	49 008	421
393	21.80	−0.19	0	17	1	–	a	69	–	–	75 113	368
394	22.10	0.46	1	28	a	a	a	83	a	a	33 358	496
395	22.40	0.16	0	22	1	a	a	76	a	–	35 109	421
396	22.70	0.13	0	22	a	a	a	66	–	a	43 497	355
397	23.00	0.29	1	25	a	–	a	83	–	–	23 165	419
398	23.30	0.35	1	26	a	–	a	74	1	a	28 243	474
399	23.36	0.11	0	21	1	–	3	73	–	–	29 897	355
400	23.42	0.97	1	43	14	–	43	10	a	–	864	82
401	23.48	–	–	–	–	–	–	–	–	–	–	–
402	23.54	–	–	–	–	–	–	–	–	17	43	6
403	23.59	–	–	–	–	–	–	–	–	–	–	–
404	23.65	–	–	–	–	–	–	–	–	–	–	–
405	23.71	–	–	–	–	–	–	–	–	–	–	–
406	23.77	–	–	–	–	–	–	–	–	–	–	–
408	23.88	0.79	1	37	–	a	a	52	–	2	1 112	95
410	24.00	0.5263	1	30	–	–	2	61	a	–	860	991

[+] Sign after Cal. age BP (kyr) refers to age model adopted from Nørgaard-Pedersen et al. (2003).
[a] Abundance < 1%.

Table 3
Core PS2138: core depth, age (kyr BP), correspondence analysis factor 1 value, calculated carbon flux, calculated paleoproductivity, 'phytodetritus species' (%), 'Atlantic species' (%), *Melonis zaandami* (%), *Cassidulina teretis*, *Fontbotia wuellerstorfi* and *Lobatula lobatula* (%), agglutinated foraminifera (%), benthic foraminifera accumulation rate (No. spec. 10 g^{-1} kyr^{-1}), number of specimens counted

Depth (cm bsf)	Cal. age BP (kyr)[+]	CAF1	C flux (g m^{-2} yr^{-1})	Paleoproductivity (g m^{-2} yr^{-1})	Phytodetritus spec. (%)	Atl. spec. (%)	*Melonis zaandami* (%)	*Cassidulina teretis* (%)	*Lobatula lobatula* and *Fontbotia wuellerstorfi* (%)	Agglutinated foraminifera (%)	WBFAR (No. spec. 10 g dry sediment^{-1} × Acc. rate kyr^{-1})	No. counted
1	0.00	1.27	2	56	a	a	11	1	–	83	638	167
2.5	0.71	1.38	2	61	–	–	a	1	–	94	3 442	558
4	1.13	1.22	1	53	a	a	–	–	–	97	1 673	318
6	1.69	1.13	1	50	–	–	a	–	a	96	612	283
10	2.82	1.41	2	62	–	–	a	–	3	91	126	76
13	3.67	1.59	2	72	–	2	5	3	1	81	87	93
17	4.80				–	–	1	5	–	63	64	29
21.5	6.35				–	–	–	–	–	–	–	–
24	6.78				–	–	2	–	–	28	66	15
27	7.62	1.75	3	81	–	1	–	–	–	62	110	42
30	8.47	2.05	4	104	–	–	1	3	–	93	152	100
32.5	9.18	1.65	2	75	–	–	16	1	–	45	33	36
35	9.88	1.09	1	47	14	12	10	–	6	–	61	154
36.5	10.45	1.21	1	52	3	5	8	14	2	4	52	87
37.5	10.73	1.00	1	44	–	–	16	11	–	16	30	40
41.5	11.72	2.39	6	135	1	–	1	20	–	80	25	43
43	12.08	1.75	3	80	–	–	6	1	–	80	36	41
46	12.55	1.47	2	64	1	–	44	–	4	16	199	43
47.5	12.86	1.00	1	44	1	1	6	–	a	1	2 012	284
51	13.33	1.31	2	56	1	–	22	80	2	2	596	508
54	13.80	1.57	2	69	2	1	9	58	a	11	1 449	311
57	14.27	1.66	2	74	a	–	8	49	a	31	747	290
60	14.74	1.55	2	67	3	a	7	68	2	9	915	410
61.5	14.97	1.31	2	55	4	a	3	68	1	6	1 947	504
71.5	15.62	1.74	3	77	3	–	12	48	4	16	7 342	422
81.5	15.77	1.35	2	56	a	–	16	65	2	5	30 998	642
92	15.93	1.28	2	53	3	–	18	70	a	2	11 526	581
101.5	16.08	0.89	1	39	3	–	2	27	6	a	21 385	566
112.5	16.47	1.46	2	61	2	a	35	13	3	15	2 579	529
122.5	17.52	0.48	1	28	4	a	a	53	2	2	22 469	527
132	18.36	0.54	1	29	2	–	a	42	3	–	40 439	539

Table 3 (*Continued*).

Depth (cm bsf)	Cal. age BP (kyr)[+]	CAF1	C flux (g m^{-2} yr^{-1})	Paleoproductivity (g m^{-2} yr^{-1})	Phytodetritus spec. (%)	Atl. spec. (%)	*Melonis zaandami* (%)	*Cassidulina teretis* (%)	*Lobatula lobatula* and *Fontbotia wuellerstorfi* (%)	Agglutinated foraminifera (%)	WBFAR (No. spec. 10 g dry sediment^{-1} × Acc. rate kyr^{-1})	No. counted
143	18.71	0.11	0	21	1	–	a	50	1	1	91 404	439
152	18.99	0.31	1	24	a	–	a	59	2	a	61 179	458
163	19.30	0.52	1	29	1	a	1	55	1	a	232 365	764
172.5	19.47	0.24	0	23	a	a	a	56	1	a	187 669	577
182.5	19.66	0.17	0	22	1	a	a	64	2	a	135 447	528
192.5	19.85	−0.11	0	17	a	–	a	62	2	a	102 798	579
203	20.21	0.38	1	26	3	a	a	32	2	1	27 636	599
213	20.94	0.32	1	24	3	a	a	32	2	1	22 948	561
223	21.68	0.18	0	22	1	–	a	63	2	a	2 530	336
233	22.31	−0.31	0	15	1	–	a	63	2	a	161 448	610
241.5	22.64	0.56	1	30	1	a	2	54	3	a	134 124	464
251	23.10	0.63	1	32	1	a	2	54	3	a	64 452	699
263	23.62	0.23	0	23	4	a	a	80	a	a	173 458	474
272.5	23.83	0.46	1	28	4	a	a	80	a	a	12 841	638

[+] Sign after Cal. age BP (kyr) refers to age model adopted from Matthiessen et al. (2001).

[a] Abundance < 1%.

WBFAR are treated as passive elements assigned to a certain CAF value. Correspondence analysis reveals only one meaningful factor (CAF1), which explains 41% of the total variance of data. The correlation between modern dead foraminiferal CAF1 values and the estimated organic carbon flux is used as transfer function for the calculation of paleo-organic C fluxes from the core CAF1 (Fig. 2). Paleoproductivities are calculated from estimated paleo-organic C fluxes using the equation of Betzer et al. (1984), after sea-level correction according to Vogelsang (1990, table A-7).

3. Results

3.1. WBFAR and carbonate dissolution

Below the Holocene usually a specimen-rich (average 67 455 spec. 10 g^{-1} kyr^{-1}) nicely preserved calcareous foraminiferal fauna, with a contribution of less than 30% agglutinants, dominates core PS2837 (Fig. 3A, Table 2). However, at the terminations of Greenland Interstadial 2 (GI-2) and GS-1 WBFAR decreases to < 100 spec. 10 g^{-1} kyr^{-1}, the relative abundance of agglutinated

Corg-Flux
$(gCm^{-2}yr^{-1})$

$$y = 0.365 * 10^{0.495x} \quad r^2 = 0.95$$
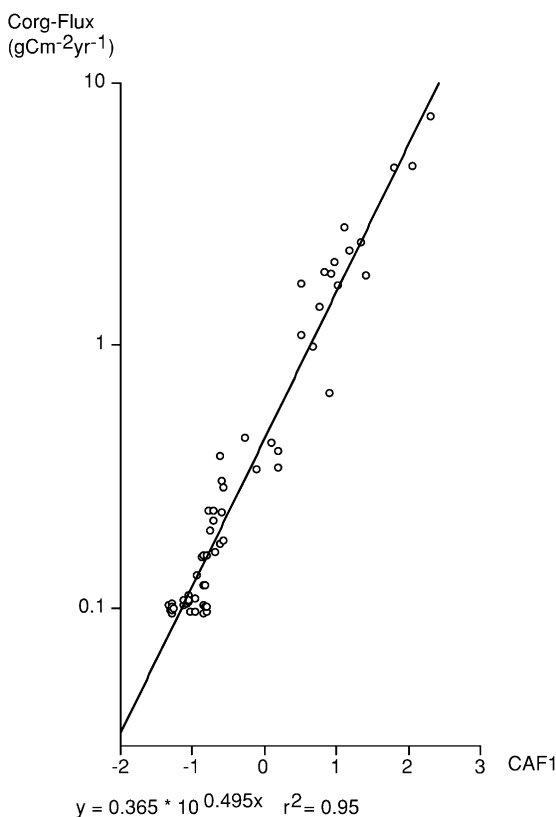
Fig. 2. CAF1 sample values of modern dead foraminifera (Wollenburg and Kuhnt, 2000), in relation to carbon flux (Appendix table 1).

foraminifera increases, whereas rare calcareous foraminifera are heavily corroded (Fig. 3A). Upper GS-1 and Holocene faunas are characterized by well-preserved calcareous, moderately abundant agglutinated foraminifera, and comparatively low WBFAR (14.82% of glacial values).

At site PS2138 glacial WBFAR (average 58 909 spec. 10 g^{-1} kyr^{-1}, Fig. 3B, Table 3) fluctuations and percentage calcareous foraminifera approximate those at site PS2837. However, in this core the drop in WBFAR at the termination of GI-2 is less significant (12 841 spec. 10 g^{-1} kyr^{-1}) than in core PS2837, and there is no drop in WBFAR in upper GI-1a. Holocene WBFAR is less than 10% of glacial values. Agglutinated foraminifera (4–97%, average 62%) dominate most faunas. Associated calcareous foraminifera are usually corroded, small-sized calcareous species usually lack-

ing. In the modern Arctic Ocean, during sea-ice formation, ejected brines create cold, saline and oxygen-rich bottom water that oxidizes labile organic matter and creates a carbonate-aggressive environment at sites with high organic matter accumulation (Steinsund and Hald, 1994). Therefore the carbonate content of sediments is at least two to three times higher under the permanent ice cover or in glacial times, than in seasonally ice-free areas or during interglacials (Pagels, 1991; Knies et al., 1999). We believe that especially GS-1 to Holocene samples of core PS2138 and samples from GI-1c–a of core PS2837 are affected by this type of carbonate dissolution (Fig. 3A,B). In such samples the abundances of 'Atlantic species' (see below) cannot be used to derive information on the presence of inflowing warm Atlantic water. However, except for such samples with less than 2% biogenic carbonate (Knies et al., 2000; Nørgaard-Pedersen et al., 2003) the abundance of Atlantic species is unrelated to carbonate dissolution.

3.2. 'Atlantic species'

The group 'Atlantic species' comprises the calcareous species *Epistominella pusilla*, *Pullenia osloensis*, *Pullenia bulloides*, *Discorbinella berthelothi* (Wollenburg et al., 2001), plus *Eggerella bradyi*, *Sigmoilopsis schlumbergeri* (Rasmussen et al., 1996), and *Siphotextularia rolshauseni* confined to glacial intervals in the study area. 'Atlantic species' sensu Wollenburg et al. (2001) are species restricted to water depths < 1200 m under the influence of the inflowing warm Atlantic water. *Sigmoilopsis schlumbergeri*, *Eggerella bradyi* and *Siphotextularia rolshauseni* are absent in the modern Arctic Ocean and Norwegian–Greenland Seas, but reveal a late Weichselian occurrence (Sejrup et al., 1984; Jansen and Erlenkeuser, 1985; Nees and Struck, 1994). Below the Holocene, these 'Atlantic species' are nearly absent in core PS2837, with the exception of upper GS-2b to lower GS-2a and GS-1, where they reach up to ~8% (Fig. 3A, Table 2). In the lower Holocene (corresponding to the time before 4.2 ka), abundances of these species are below 1%, with the exception of values of 2–4% in the sediments cor-

responding in time to 9.7–8.2 ka. The species are present again between 4.2 ka and 100 yr BP, at fluctuating values of up to 2–4%. Over the last 100 yr the 'Atlantic species' constituted less than 1% of the assemblage. In core PS2138 the abundance of the 'Atlantic species' is usually below 1%, with the exception of values of up to 12% in two samples dated at 9.9–10.5 ka (Fig. 3B, Table 3).

3.3. Paleoproductivity estimations in the marginal eastern Arctic Ocean

The composition and standing stock of the bentho-pelagic and epibenthic fauna is related to primary production or more precisely the amount of carbon that reaches the bathyal benthic boundary layer. Yet the processes governing the transfer of material to the seafloor are still not fully understood (Wefer, 1993). Early studies proposed a linear relationship between primary production and carbon flux (Suess, 1980). However, modern studies showed that the relative export production is lower in oligotrophic oceans, and higher in areas with strong seasonally productive blooms (Berger et al., 1989; Berger and Wefer, 1990, 1992; Lampitt and Antia, 1997). Subsequent studies proposed exponential equations to relate primary production to carbon flux (Betzer et al., 1984; Pace et al., 1987; Martin et al., 1987; Schlüter et al., 2000). Due to the lack of equations to relate Arctic primary production to carbon flux, we applied the equations of Schlüter et al. (2000) from the adjacent northern North Atlantic (60–80°N), Suess (1980), Betzer et al. (1984) and Pace et al. (1987) from lower latitudes in the Pacific Ocean, to calculate 'estimated carbon fluxes'. 'Estimated carbon fluxes' calculated by the equation of Suess (1980) are generally higher than those of Betzer et al. (1984) and Pace et al. (1987), but show an about equal exponential increase with CAF1 values (Fig. 5). In contrast the function of Schlüter et al. (2000) is very steep, reflecting their assumption that only a fraction of 1.7–1.8% of primary produced organic carbon is transferred to the seafloor. In contrast, in the Gulf of St. Lawrence the mean annual export production is 35% of primary production (Vézina et al., 2000), supporting

the assumption of an enhanced export ratio suggested for high latitudes (Buesseler, 1998). Moreover, due to the steep increase in estimated carbon flux with CAF1 values (Fig. 5), the transfer function deduced from the equation of Schlüter et al. (2000) is extremely sensitive to faunal changes. Because Arctic sediment cores are always affected by carbonate dissolution, bacterial activity, or bioturbation, we preferred a more robust transfer function. Within the range of the modern primary production data set, all transfer functions produce comparable results (Fig. 5). However, results differ when paleoproductivity exceeds modern core site primary production values. This study uses the equation of Betzer et al. (1984) because the calculated paleoproductivities are obviously minimum estimates (Fig. 5). Although the mean primary production values assigned to our surface samples may not match the real values of each site, the relation to the site foraminiferal fauna is reasonable. The correlation coefficient between estimated carbon flux and modern CAF1 values is $r^2 = 0.954$, the error between input data and values calculated by applying the transfer function ± 20%.

The reliability of paleoproductivity estimates demands approximate modern analog sediment core faunas preferably unaffected by bioturbation. Apart from peak glacial intervals (indicated by minimum paleoproductivities), during which burrows are absent, bioturbation is moderate in both cores (M. Pirrung, personal communication, 2001). However, sedimentation rate in the study area is usually < 36 cm kyr^{-1}, suggesting that bioturbation is included in both modern surface and sediment core samples.

For most of the GS-1 to Holocene at site PS2138 and during certain intervals at site PS2837 the foraminiferal faunas are dominated by agglutinated taxa. This is a common phenomenon in Arctic waters with high organic matter accumulation and on the one hand is caused by an increased abundance of agglutinated species living at such sites (Wollenburg and Kuhnt, 2000). On the other hand the thanatocoenosis is usually affected by the prevailing carbonate-corrosive conditions mentioned above. However, because this type of carbonate dissolution is almost

A PS2837

▼ AMS 14C datings, age model of core PS2837 adopted from Nørgaard-Pedersen et al. (2002)

----- Event chronology proposed by the integration of ice-core, marine and terrestrial records (INTIMATE) group (Björck et al., 1998) dated according to the Gisp2 ice-core record (Cacho et al., 2001). GS = Greenland (Isotope) Stadial, GI = Greenland (Isotope) Interstadial, YD = Younger Dryas, B-A = Bølling-Allerød, LGM = Last Glacial Maximum

········ Nordway events (NE) (Hebbeln and Wefer, 1997)

▧ Carbonate dissolution intervalls

Fig. 3. WBFAR (No. spec. 10 g^{-1} kyr^{-1}), agglutinated versus calcareous foraminifera (%), 'Atlantic species' (%), *Cassidulina teretis* (%), 'phytodetritus species' (%), *Melonis zaandami* (%), and *Fontbotia wuellerstorfi* and *Lobatula lobatula* (%) for (A) core PS2837 and (B) core PS2138.
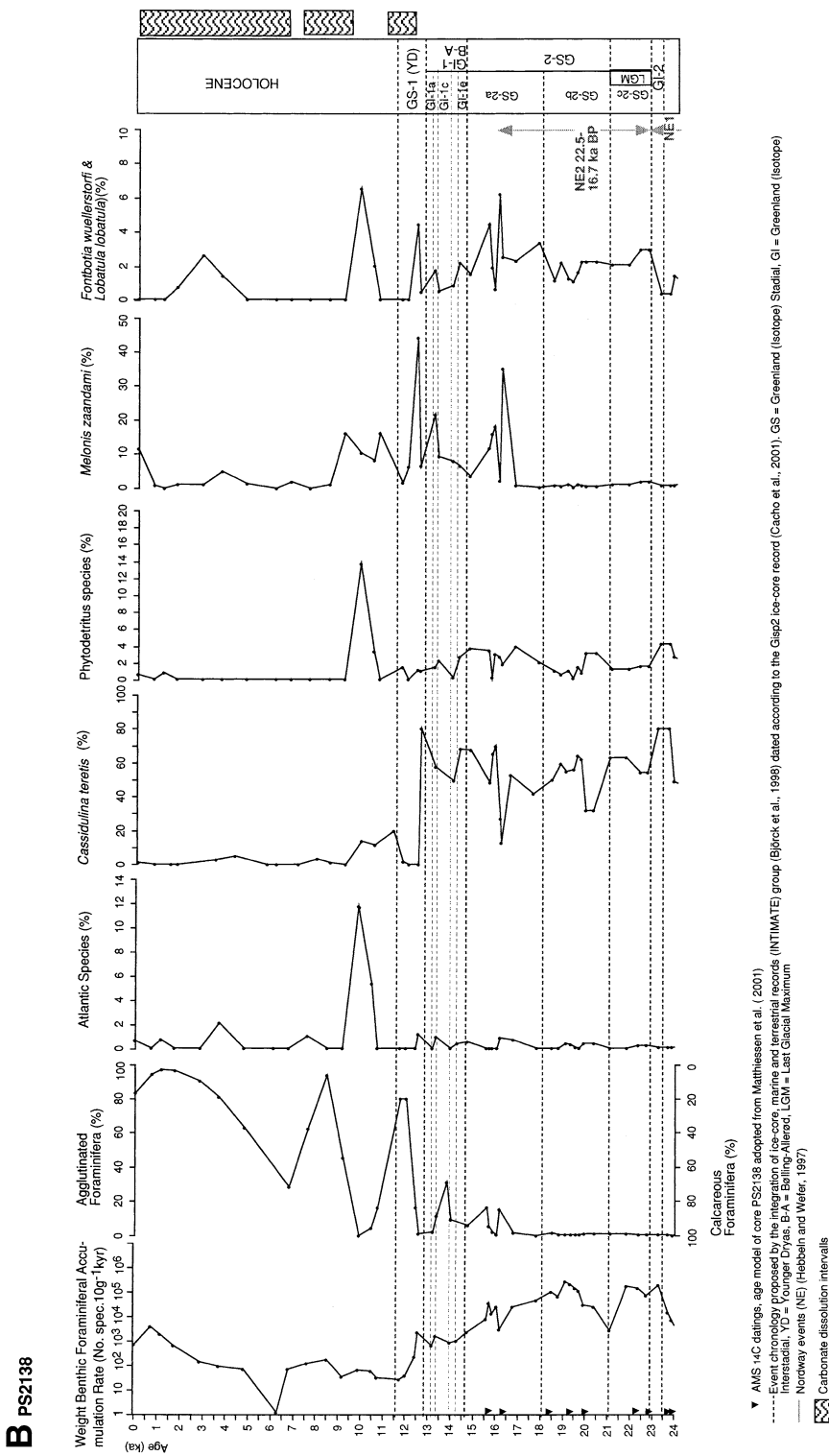
Fig. 3 (*Continued*).
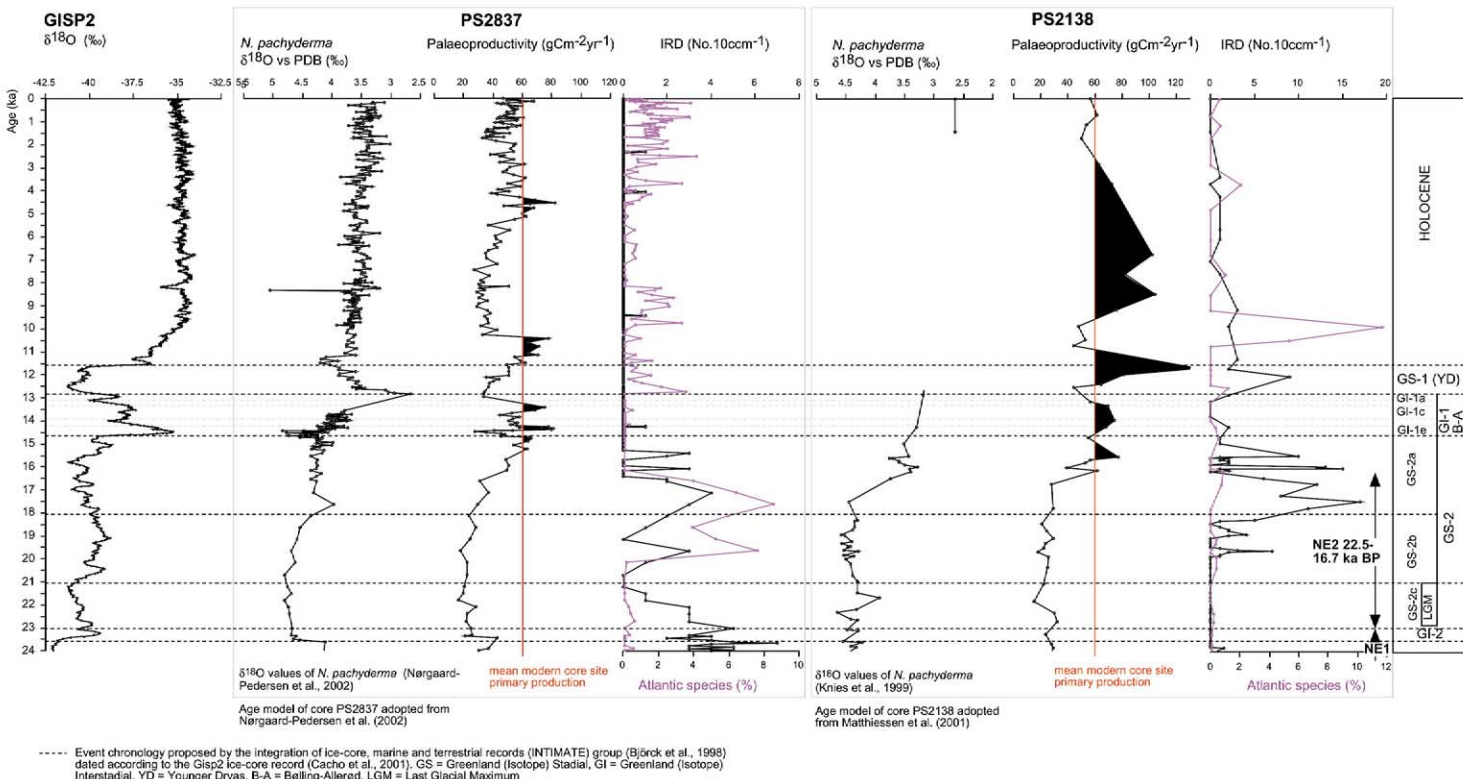
Fig. 4. GISP2: $\delta^{18}O$ (‰) values. Cores PS2837 and PS2138: $\delta^{18}O$ (‰ PDB) values of *Neogloboquadrina pachyderma*, calculated paleoproductivity, IRD (10 ccm^{-1}), and percentage of 'Atlantic species' (%).
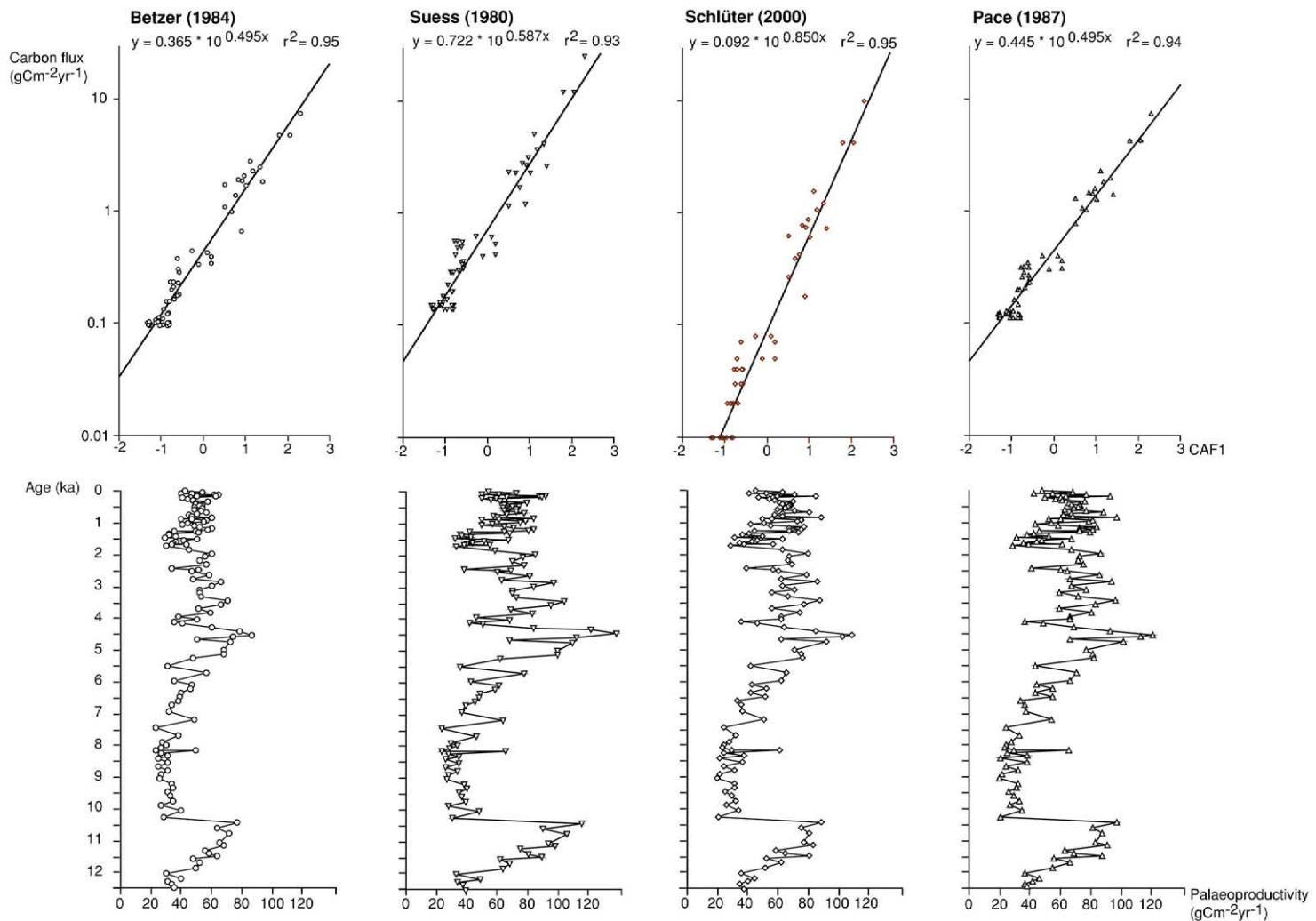
Fig. 5. Comparison of different empirical relationships: calculated carbon flux from modern primary production data. Applying the established transfer functions to core PS2837.

exclusively restricted to the topmost centimeter in the study area (J.E. Wollenburg, personal observation) it is likewise included in the modern data set. This makes the use of modern acid-treated assemblages for comparison with sediment core samples as proposed by Murray and Alve (1994) and Alve and Murray (1995) unnecessary, for this study. Furthermore the habitats of all 15 calcareous and 10 agglutinated species with scores above 1.0 (values of a species on an ordination axis, center of species curve) are restricted to seasonally ice-free areas, suggesting that the significance of agglutinated species for paleoproductivity estimates is unrelated to carbonate dissolution.

3.4. Correspondence analysis and paleoproductivity

In the modern Arctic Ocean, relatively highly productive sites are dominated by agglutinated (e.g. *Astrorhizoides polygonus*, *Atlantiella atlantica*, *Cribrostomoides jeffreysii*, *Deuterammina D. grisea*, *Reophax* spp., *Recurvoides* spp., *Portatrochamina karica*, *Textularia torquata*) and calcareous (e.g. *Angulogerina fluens*, *Bolivina pseudopunctata*, *Buccella* spp., *Epistominella pusilla*, *Fursenkoina fusiformis*, *Nonionella* spp., *Nonionellina labradorica*, *Islandiella* spp., *Rosalina wrightii*, *Rupertina stabilis*, *Melonis zaandami*, *Lobatula lobatula*) species (Wollenburg and Kuhnt, 2000). These species have the highest species scores in correspondence analyses. The significance of all species is shown in Appendix Table 5.

At site PS2837, paleoproductivity was about a third to half of present values ($\sim$60 g C m^{-2} yr^{-1}) before 18 ka (GS-2b and earlier) (Fig. 4, Table 2). It then increased through GS-2a until it reached values slightly above those of the present. During GI-1e–a values fluctuated strongly, with peaks higher than today's values in upper GI-1e and upper GI-1c. Thereafter an increasing dominance of *Reophax scorpiurus* and *Reophax subfusiformis* on the one hand reflects intense carbonate dissolution, on the other hand indicates persisting high paleoproductivities until the onset of GS-1. However, low WBFAR and a subsequent barren interval impede paleoproductivity analyses for the period 13.3–12.9 ka at site PS2837. During GS-1 values increased from

about 40 to 60 g C m^{-2} yr^{-1}. Between 11.5 and 10.5 ka values were higher than today, followed by a sudden drop at 10.5 ka. Throughout the Holocene values were similar to today's, with the exception of a peak of about 60–80 g C m^{-2} yr^{-1} between 4.4 and 5.5 ka. The glacial productivity in core PS2138 resembled that in core PS2837, as far as can be ascertained because of the lower resolution of the data from the former core. A major difference is the high productivity values in GS-1 (up to 125 g C m^{-2} yr^{-1}) in core PS2138 (Fig. 4, Table 3).

4. Discussion

4.1. Paleontological indicators of Atlantic water

In the modern Arctic Ocean the abundance of 'Atlantic species' is highest close to Fram Strait, and decreases eastwards (Wollenburg et al., 2001). These species are relatively abundant in cores under WSC, and are not present where this water mass has lost much of its heat and salt because of mixing, and sinks below a 200-m-thick low-salinity surface layer on its way to the Siberian shelves (see Rudels et al., 1994). However, it is not clear which parameters restrict the habitat of 'Atlantic species' to areas under the influence of the WSC. If it were solely the availability of food, 'Atlantic species' should be more abundant in the Chukchi Sea than off Spitsbergen. But these species are absent in the Chukchi Sea (Osterman et al., 1999), and in the Laptev and East Siberian Seas (Wollenburg, unpublished data), suggesting these species need the higher temperatures and/or salinities of the WSC. Strong advection of Atlantic waters in the WSC as in the present ocean leads to increased seasonal productivity, occasionally high rates of accumulation of organic carbon, and thus severe carbonate dissolution (as at site PS3138). Under these conditions the carbonate tests of the Atlantic species dissolve, and they thus cannot be used to indicate the presence/absence of WSC. In samples with less than 1–2% biogenic carbonate data on dinoflagellates and/or macerals then may be used to indicate the presence/absence of WSC (Kunz-Pirrung, 1998; Ro-

chon et al., 1999; Boucsein et al., 2000; Matthiessen et al., 2001).

Cassidulina teretis has a circum-Arctic distribution in water depths between 200 and 1400 m. It is therefore used as an indicator for the presence of Atlantic water in most benthic foraminiferal studies (e.g. Polyak, 1990; Bergsten, 1994; Polyak and Solheim, 1994; Ishman and Foley, 1996; Hald et al., 1999; Lubinski et al., 2001). However, the exact nature of the relationship between *C. teretis* and Atlantic water is still unclear (Osterman et al., 1999). Mackensen and Hald (1988) regard *C. teretis* as a temperature-sensitive species with a common distribution in the temperature range of −1 to 2°C. With the exception of Fram Strait and northwestern Spitsbergen, where the temperatures of inflowing Atlantic water masses exceed +2°C, all Arctic water masses fall in this temperature range (e.g. Rudels et al., 2000). Yet, living *C. teretis* are rare or absent in the permanently ice-covered Eurasian Basin, and its abundance along the continental slopes is unrelated to the eastward diminishing influence of WSC (Wollenburg and Kuhnt, 2000). Moreover, during the last glacial, the stable maxima of *C. teretis* would imply a persistent Atlantic water inflow that presumably exceeded its modern volume, a finding that contradicts previous sedimentological, paleontological and oxygen isotope studies (Fig. 3A,B; e.g. Hebbeln and Wefer, 1997; Nørgaard-Pedersen et al., 1998; Matthiessen et al., 2001). *Cassidulina teretis* may probably feed on bacteria linked to seasonal carbon fluxes in the North Atlantic (Gooday and Lambshead, 1989) and perhaps the Arctic Ocean (Kröncke et al., 1994). Therefore, high abundances of *C. teretis* during glacial intervals may be an indication of not permanently ice-covered conditions. However, periodically ice-free conditions are not necessarily linked to a warm Atlantic water advection. Catabatic winds from glacial ice sheets or surface ocean circulation patterns may have caused leads or polynyas in the near-coast glacial sea ice (e.g. Knies et al., 1999).

4.2. Seasonality and maximum paleoproductivity

Epistominella exigua and *Epistominella pusilla* are known to feed on, and reproduce in phase with, seasonal pulses of freshly accumulated phytodetritus (Gooday, 1994; Smart et al., 1994). A similar behavior is assumed for *Islandiella helenae* and *Islandiella norcrossi* in the Arctic Ocean (Wollenburg, unpublished data). Such 'phytodetritus species' (Gooday, 1994; Smart et al., 1994; Thomas et al., 1995) are found in most carbonate-bearing samples, and, like *Cassidulina teretis*, reflect sustained seasonal production pulses and non-permanently ice-covered conditions at both core sites during the last 24 kyr (Fig. 3A,B, Tables 2 and 3).

Where nutrients are enriched, as in the Chukchi Sea, or replenished by upwelling or riverine input, Arctic primary production may significantly exceed 300 g C m^{-2} yr^{-1} (Springer and McRoy, 1993; Lara et al., 1994; Grebmeier, 1993; Smith et al., 1995, 1997; Grebmeier et al., 1995). Yet in the modern study area a strong vertical stratification of the water column hinders a diffusive nutrient replenishment of Arctic surface waters by intermediate deep Atlantic waters. In contrast, heavy oxygen isotope values of *Neogloboquadrina pachyderma* (Knies et al., 1999; Nørgaard-Pedersen et al., 2003) may indicate that this vertical stratification was somewhat weaker during peak glacial times. Therefore, during initial deglaciations, shear stress between wind-induced sea-ice drift and the waning ice sheets or exposed shelf may lead to the development of leads and polynyas along the continental slope. At such glacial seasonally ice-free sites upwelling processes, nutrient influx by melting sea ice, calving ice sheets, draining rivers, and atmospheric transport may have supported algal growth.

4.3. The history of Atlantic water inflow and paleoproductivity during the last 24 kyr at sites off Spitsbergen and the Barents Sea

It is assumed that glacial seasonally ice-free conditions in the Nordic Seas and Fram Strait were essentially restricted to temperate Atlantic surface water advections, the Nordway events (Hebbeln et al., 1994; Dokken and Hald, 1996; Hald et al., 1996; Hebbeln and Wefer, 1997). Glacial occurrences of 'Atlantic species' are almost

confined to Nordway event 2 (22.5–16.7 cal. kyr BP; Hebbeln and Wefer, 1997; Fig. 3A,B, Tables 2 and 3). Whereas, during the initial Nordway event 2, seasonally ice-free waters provided moisture for the GS-2c Svalbard–Barents Sea ice-sheet advance to the shelf edge (at 20–19 ^{14}C ka; Vorren and Laberg, 1996; Lambeck, 1995; Knies et al., 2000; Sarnthein et al., 2000), from upper GS-2b to lower GS-2a peaks in 'Atlantic species' preceding or in coincidence with peaks in IRD suggest that the advection of warm Atlantic water either led to or coincided with initial ice-sheet instabilities. Finally low δ^{18}O spikes of planktonic foraminifera characterize the Svalbard–Barents Sea ice-sheet retreat since $\sim$18 kyr BP (e.g. Elverhøi et al., 1995; Mangerud et al., 1996; Landvik et al., 1998; Nørgaard-Pedersen et al., 1998; Sarnthein et al., 2000; Knies et al., 1999; Figs. 4 and 6). Coinciding with the increasing meltwater

influx (e.g. Jones and Keigwin, 1988; Stein et al., 1994; Dokken and Hald, 1996; Nørgaard-Pedersen et al., 1998; Hald et al., 2001) rare or absent 'Atlantic species' indicate a period of diminished or cold Atlantic water advection from 16 to 14 kyr BP (Hebbeln and Wefer, 1997).

The GS-1 cooling led to a renewed advance of the Svalbard–Barents Sea ice sheet (e.g. Landvik et al., 1998, Fig. 6). A coeval drop in δ^{18}O values of planktonic foraminifera is attributed to a sudden freshwater influx from the Lena river (Sarnthein et al., 2000; Nørgaard-Pedersen et al., 2003). However, the summer salt transport and inner momentum of the thermohaline circulation were obviously strong enough to maintain a Holocene-type circulation pattern in the Nordic Seas (Sarnthein et al., 2000). A peak in 'Atlantic species', coincident with the meltwater spike at the onset of GS-1, corroborates this assumption in this
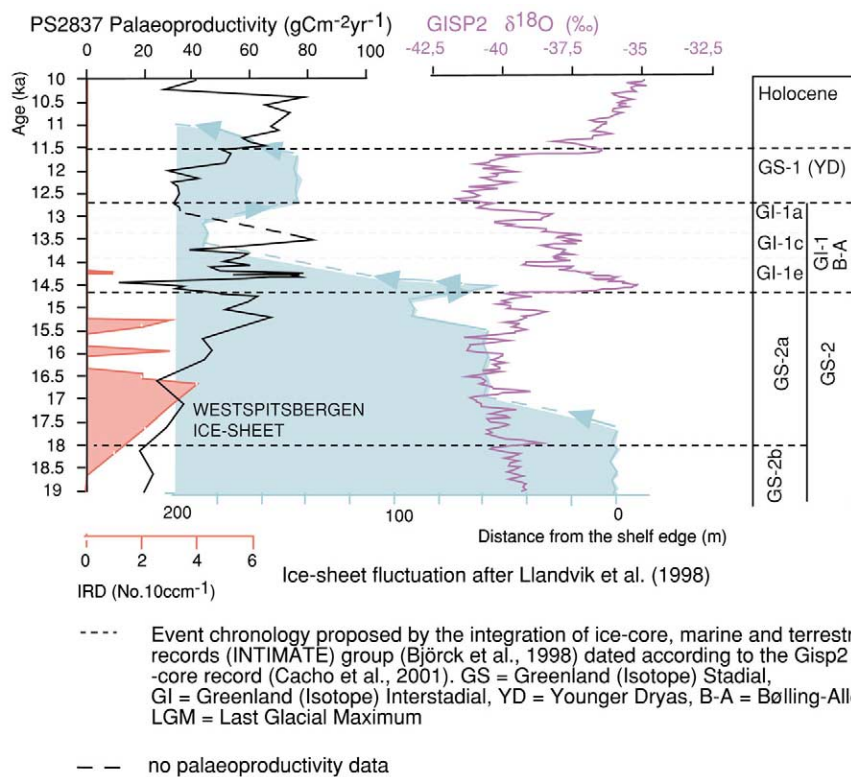
Fig. 6. Comparison of the deglacial West Spitsbergen ice-sheet fluctuations (after Landvik et al., 1998) with coincident paleoproductivity fluctuations at site PS2837.

study (Fig. 4). Thereafter, the abundance of 'Atlantic species' decreased towards the onset of the Holocene.

It has been previously suggested that the advection of Atlantic water into the Nordic Seas was stronger than today during the lower to middle Holocene (Polyak and Mikhailov, 1996). An enhanced advection of temperate Atlantic water is indicated for the period before the 8.2 ka cold event (Alley et al., 1997) by grain size analyses (Hass, personal communication, 2001) and stable high abundances of 'Atlantic species' (10–8.2 ka, Fig. 3A). Thereafter absent or rare 'Atlantic species', ostracod species (Cronin et al., 1994, 1995)

and more fine-grained sediments (Hass, personal communication, 2001) indicate a period of reduced Atlantic water advection until 5.2 ka. Fluctuating abundances of 'Atlantic species' characterize the remaining Holocene.

Glacial and early Holocene peak paleoproductivity occurred during periods of retreat of the Svalbard–Barents Sea ice sheet, which were usually coeval with warm periods in the GISP2 ice-core record retreat, and low oxygen isotope values in planktonic foraminifera (correlation coefficient $r^2 = 0,54$) (Grootes et al., 1993; Stein et al., 1994; Nørgaard-Pedersen et al., 1998; Knies et al., 1999; Poore et al., 1999; Moore et al., 2000;
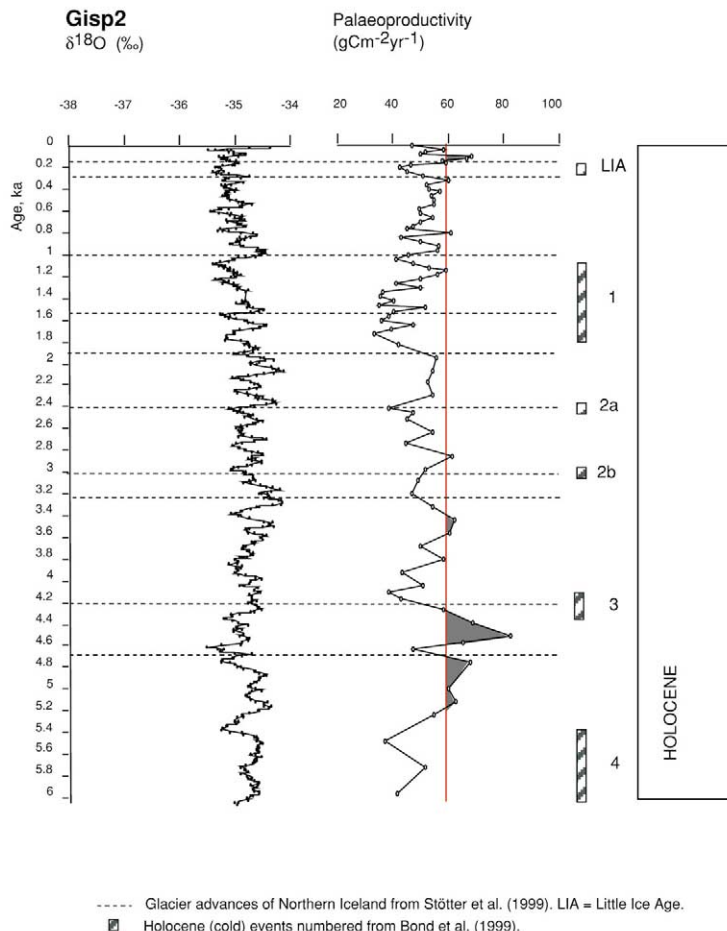
Fig. 7. Holocene section of core PS2837: paleoproductivity versus GISP2 δ^{18}O (‰) values, glacier advances and Holocene ice-rafting events.

Sarnthein et al., 2000; Nørgaard-Pedersen et al., 2002; Figs. 4 and 6). Paleoproductivities are reduced to about a third of their modern level during the maximum Svalbard–Barents Sea ice-sheet extensions, coeval with cold periods in the GISP2 ice-core record, and heavy oxygen isotope values in planktonic foraminifera (Figs. 4 and 6). These reduced paleoproductivity values are still higher than values for modern, permanently ice-covered regions, suggesting that the core locations were at least partially ice-free, as also suggested by a low relative abundance of 'phytodetritus species' and peak abundances of *Cassidulina teretis* (Fig. 4, Tables 2 and 3).

After the terminal deglaciation (10.7–9.1 kyr BP; Polyak and Mikhailov, 1996; Hald and Aspeli, 1997; Hald et al., 1999), paleoproductivities decreased to half and two thirds of their modern values at sites PS2837 and PS2138, respectively (Fig. 4). During the Holocene Climatic Optimum paleoproductivities were high at the Barents Sea site, but much lower than at present on the Yermak Plateau, perhaps because of different effects of an enhanced Atlantic water advection (Polyak and Mikhailov, 1996; Duplessy et al., 2001; see also above). Whereas a stronger than today NSC may have enhanced the seasonal ice retreat and thus primary production at site PS2138, a counterbalancing broadened East Greenland Current may have increased the sea-ice coverage and lowered primary production at site PS2837 (Fig. 1). However, at site PS2837 coincident maxima in *Fontbotia wuellerstorfi*/*Lobatula lobatula*, related to current activities of organic matter-enriched water masses (Linke and Lutze, 1993), and *Melonis zaandami*, related to high fluxes of slightly altered organic matter (Caralp, 1989), suggest an allochthonous food source, e.g. along-slope or down-slope transport of slightly altered organic matter. The most likely source of this altered organic matter is an increased shelf production close to the Yermak Plateau (see also Polyak and Mikhailov, 1996). Since the establishment of modern-type hydrographic conditions at ∼5 kyr BP (Polyak and Mikhailov, 1996) both core sites reveal comparable paleoproductivity fluctuations (Fig. 4). The high-resolution data set from site 2837 documents that the late Holocene paleopro-

ductivity decreased during cold periods such as the Little Ice Age (16th to 19th century), periods of glacier advances, enhanced ice-rafting and cooler, fresher surface waters in the North Atlantic (Stötter et al., 1999; Bond et al., 1997, 2000; Fig. 7). Upper Holocene peak paleoproductivities exceeding the modern core site production from 5.2 to 4.4 ka (only site PS2837), and around 2.8 ka (both core sites) are concomitant with the occurrence of thermophilic molluscs in the adjacent Kara Sea (Hald et al., 1999).

5. Conclusions

Foraminiferal analyses in cores taken at about 1000 m water depth, adjacent to the former, LGM Svalbard–Barents Sea ice-sheet edge, reveal significant paleoproductivity fluctuations during the waxing and waning of the ice sheet. Paleoproductivity was reduced to about one third of its present level during glacial stadials. These reduced values are still higher than values for modern, permanently ice-covered regions. Together with high glacial abundances of *Cassidulina teretis*, this is a distinct indication for a spatio-temporarily reduced seasonal sea-ice retreat. Paleoproductivities exceeding those of the modern core site production characterize initial deglaciations (upper GS-2a, lower Holocene) and warm sub-stages within GI-1. Peak deglacial paleoproductivities occur in samples with low $\delta^{18}O$ values of planktonic foraminifera, yet subsequent to peak abundances of 'Atlantic species', suggesting that the final build-up and initial Svalbard–Barents Sea ice-sheet retreat was initiated or supported by an enhanced advection of warm Atlantic-derived water.

During the Holocene Climatic Optimum paleoproductivity was reduced by one third its modern value at the Yermak Plateau, higher than today at the Barents Sea site, perhaps because of increased advection of Atlantic water to the latter site and heavier ice coverage at the former. Since 5.4 ka paleoproductivities at both sites have been similar. However, cold events like the Little Ice Age left their imprint by significantly reducing paleoproductivities.

Acknowledgements

References

Alley, R., Mayewski, P.A., Sowers, T., Stuiver, M., Taylor, K.C., Clark, P.U., 1997. Holocene climate instability: a prominent widespread event 8200 y ago. Geology 25, 483–486.

Alve, E., Murray, J.W., 1995. Benthic foraminiferal distribution and abundance changes in Skagerrak surface sediments: 1937 (Höglund and 1992/1993 data compared). Mar. Micropalaeontol. 25, 269–288.

Antoine, D., André, J.-M., Morel, A., 1996. Oceanic primary production: 2. Estimation at global scale from satellite (coastal zone color scanner) chlorophyll. Global Biogeochem. Cycles 10, 57–69.

Are, F.E., 1999. The role of coastal retreat for sedimentation in the Laptev Sea. In: Kassens, H., Bauch, H.A., Dmitrenko, I.A., Eicken, H., Hubberten, H.-W., Melles, M., Thiede, J., Timokhov, L.A. (Eds.), Land-Ocean Systems in the Siberian Arctic: Dynamics and History. Springer-Verlag, Berlin, pp. 287–295.

Belkin, I.M., Levitus, S., Antonov, J., Malmberg, S.-A., 1998. 'Great salinity anomalies' in the North Atlantic. Prog. Oceanogr. 41, 1–68.

Berger, W.H., Wefer, G., 1990. Export production: Seasonality and intermittency, and paleoceanographic implications. Palaeogeogr. Palaeoclimatol. Palaeoecol. 89, 245–254.

Berger, W.H., Wefer, G., 1992. Flux of biogenous materials to the seafloor: Open questions. In: Hsü, K.J., Thiede, J. (Eds.), Use and Misuse of the Seafloor, Wiley, New York, 285–304.

Berger, W.H., Smetacek, V., Wefer, G., 1989. Ocean productivity and paleoproductivity – An Overview. In: Berger, W.H., Smetacek, V., Wefer, G. (Eds.), Productivity of the Ocean: Present and Past. Dahlem Workshop Reports, Wiley, New York, 1–34.

Bergsten, H., 1994. Recent benthic foraminifera of a transect from the North Pole to the Yermak Plateau, eastern central Arctic Ocean. Mar. Geol. 119, 251–267.

Betzer, P.R., Showers, W.J., Laws, E.A., Winn, C.D., DiTullio, G.R., Kroopnick, P.M., 1984. Primary productivity and particle fluxes on a transect of the equator at 153°W in the Pacific Ocean. Deep-Sea Res. 31, 1–11.

Björck, S., Walker, M.J.C., Cwynar, L.C., Johnsen, S., Knudsen, K.-L., Lowe, J.J., Wohlfarth, B., INTIMATE Members, 1998. An event stratigraphy for the Last Termination in the North Atlantic region based on the Greenland ice-core record: a proposal by the INTIMATE group. J. Quat. Sci. 13, 283–292.

Boetius, A., Grahl, C., Kröncke, I., Liebezeit, G., Nöthig, E.-M., 1996. Distribution of plant pigments in surface sediment of the Eastern Arctic. In: Stein, R., Ivanov, G.I., Levitan, M.A., Fahl, K. (Eds.), Surface-Sediment Composition and Sedimentary Processes in the Central Arctic Ocean and along the Eurasian Continental Margin. Ber. Polarforsch. 212, 213–218.

Boetius, A., Damm, E., 1998. Benthic oxygen uptake, hydrolytic potentials and microbial biomass at the Arctic continental slope. Deep-Sea Res. I 45, 239–275.

Bond, G., Showers, W., Cheseby, M., Lotti, R., Almasi, P., deMenocal, P., Priore, P., Cullen, H., Hajdas, I., Bonani, G., 1997. A pervasive millennial-scale cycle in North Atlantic Holocene and glacial climates. Science 278, 1257–1266.

Bond, G.C., Showers, W., Elliot, M., Evans, M., Lotti, R., Hajdas, I., Bonani, G., Johnson, S., 2000. The North Atlantic's 1–2 kyr climate rhythm: Relation to Heinrich Events, Dansgaard/Oeschger Cycles and the Little Ice Age. In: Clark, P.U., Webb, R.S., Lloyd, D.K. (Eds.), Mechanisms of Global Climate Change at Millennial Time Scales. Geophys. Monogr. 112, 35–58.

Boucsein, B., Stein, R., 2000. Particulate organic matter in surface sediments of the Laptev Sea (Arctic Ocean): application of maceral analysis as organic-carbon-source indicator. Mar. Geol. 162, 573–586.

Boucsein, B., Fahl, K., Stein, R., 2000. Variability of river discharge and Atlantic-water inflow at the Laptev Sea continental margin during the past 15,000 years: implications from maceral and biomarker records. Int. J. Earth Sci. 89, 578–591.

Buesseler, K.O., 1998. The decoupling of production and particulate export in the surface ocean. Global Biogeochem. Cycles 12, 297–310.

Caralp, M.H., 1989. Abundance of *Bulimina exilis* and *Melonis barleeanum*: Relationship to the quality of marine organic matter. Geo-Mar. Lett. 9, 37–43.

Carstens, J., Wefer, G., 1992. Recent distribution of planktonic foraminifera in the Nansen Basin, Arctic Ocean. Deep-Sea Res. 30, 507–524.

CLIMAP, 1981. Seasonal reconstructions of the Earth's surface at the Last Glacial Maximum. Map and chart series. Geol. Soc. Am. MC-36-1981.

Clough, L.M., Ambrose, W.G.Jl., Cochran, J.K., Barnes, C., Renaud, P.E., Aller, R.C., 1997. Infaunal density, biomass and bioturbation in the sediments of the Arctic Ocean. Deep-Sea Res. II 44, 1683–1704.

Cota, G.F., Legendre, L., Gosselin, M., Ingram, R.G., 1991. Ecology of bottom ice algae: I. Environmental cotrols and variability. J. Mar. Syst. 2, 257–277.

Cota, G.F., Pomeroy, L.R., Harrison, W.G., Jones, E.P., Pe-

ters, F., Sheldon, W.M., Weingartner, T.R., 1996. Nutrients, primary production and microbial heterotrophy in the southeastern Chukchi Sea: Arctic summer nutrient depletion and heterotrophy. Mar. Ecol. Prog. Ser. 135, 247–258.

Cronin, T.M., Holtz, T.R., Jr., Whatley, R.C., 1994. Quaternary paleoceanography of the deep Arctic Ocean based on quantitative analysis of Ostracoda. Mar. Geol. 119, 305–332.

Cronin, T.M., Holtz, T.R., Jr., Stein, R., Spielhagen, R., Fütterer, D., Wollenburg, J., 1995. Late Quaternary paleoceanography of the Eurasian Basin, Arctic Ocean. Paleoceanography 10, 259–281.

Dickson, R.R., Meincke, J., Malmberg, S.-A., Lee, A.J., 1988. The 'Great Salinity Anomaly' in the northern North Atlantic 1968–1982. Prog. Oceanogr. 20, 103–151.

Dokken, T.M., Hald, M., 1996. Rapid climatic shifts during isotope stages 2–4 in the Polar North Atlantic. Geology 24, 599–602.

Duplessy, J.-C., Ivanova, E., Murdmaa, I., Paterne, M., Labeyrie, L., 2001. Holocene paleoceanography of the northern Barents Sea and variations of the northward heat transport by the Atlantic Ocean. Boreas 30, 2–16.

Elverhøi, A., Dokken, T., Hebbeln, D., Spielhagen, R., Svendsen, J.I., Søflaten, M., Rørnes, A., Hald, M., Forsberg, C.F., 1995. The growth and decay of the late Weichselian ice-sheet in western Svalbard and adjacent areas based on provenance studies of marine sediments. Quat. Res. 44, 303–316.

English, T.S., 1961. Some Biological Oceanographic Observations in the Central North Polar Sea. Drift Station ALPHA, 1957–1958. Arct. Inst. N. Am. Res. Pap. 13.

Fahl, K., Stein, R., 1999. Modern organic-carbon-deposition in the Laptev Sea and the adjacent continental slope: surface-water productivity vs terrigenous input. Org. Geochem. 26, 379–390.

Forman, S.L., Lubinski, D.J., Miller, G.H., Matishov, G., Snyder, J., Korsun, S., 1995. Postglacial emergence and distribution of Late Weichselian ice-sheet loads in the Northern Barents and Kara Seas, Russia. Geology 23, 113–116.

Gard, G., 1993. Late Quaternary coccoliths at the North Pole: evidence of ice free conditions and rapid sedimentation in the central Arctic Ocean. Geology 21, 227–230.

Gooday, A.J., Lambshead, P.J.D., 1989. Influence of seasonally deposited phytodetritus on benthic Foraminifera populations in the bathyal northeast Atlantic: the species response. Mar. Ecol. Prog. Ser. 58, 53–67.

Gooday, A.J., 1994. Deep-sea benthic foraminiferal species which exploit phytodetritus: Characteristic features and controls on distribution. Mar. Micropaleontol. 22, 187–205.

Gosselin, M., Levasseur, M., Wheeler, P.A., Horner, R.A., Booth, B.C., 1997. New measurements of phytoplankton and ice algal production in the Arctic Ocean. Deep-Sea Res. II 44, 1571–1592.

Grebmeier, J.M., 1993. Studies of pelagic-benthic coupling extending onto the Soviet continental shelf in the northern Bering and Chukchi Seas. Cont. Shelf Res. 13, 653–668.

Grebmeier, J.M., Smith, W.O., Conover, R.J., 1995. Biological processes on Arctic continental shelves: ice-ocean-biotic interactions. Coast. Estuar. Stud. 49, 231–261.

Green, K.E., 1960. Ecology of some Arctic foraminifera. Micropalaeontology 6, 57–78.

Grootes, P.M., Stuiver, M., White, J.W.C., Johnsen, S., Jouzel, J., 1993. Comparison of oxygen isotope records from the Gisp 2 and GRIP Greenland ice cores. Nature 366, 552–554.

Hald, M., Aspeli, R., 1997. Rapid climatic shifts of the northern Norwegian Sea during the last deglaciation and the Holocene. Boreas 26, 15–28.

Hald, M., Steinsund, P.I., 1996. Benthic foraminifera and carbonate dissolution in surface sediments of the Barents- and Kara Sea. In: Stein, R., Ivanov, G.I., Levitan, M.A., Fahl, K. (Eds.), Surface-Sediment Composition and Sedimentary Processes in the Central Arctic Ocean and along the Eurasian Continental Margin. Ber. Polarforsch. 212, 285–307.

Hald, M., Dokken, T., Hagen, S., 1996. Palaeoceanography on the European Arctic margin during the last deglaciation. In: Andrews, J.T., Austin, W.E.N., Bergsten, H., Jennings, A.E. (Eds.), Late Quaternary Palaeoceanography of the North Atlantic Margins. Geol. Soc. Spec. Publ. III, 275–289.

Hald, M., Kolstad, V., Polyak, L., Forman, S.L., Herlihy, F.A., Ivanov, G., Nescheretov, A., 1999. Late-glacial and Holocene paleoceanography and sedimentary environments in the St. Anna Trough, Eurasian Arctic Ocean margin. Palaeogeogr. Palaeoclimatol. Palaeoecol. 146, 229–249.

Hald, M., Dokken, T., Mikalsen, G., 2001. Abrupt climate change during the last interglacial-glacial cycle in the polar North Atlantic. Mar. Geol. 176, 121–137.

Hebbeln, D., Dokken, T., Andersen, E.S., Hald, M., Elverhøi, A., 1994. Moisture supply for northern ice-sheet growth during the Last Glacial Maximum. Nature 370, 357–360.

Hebbeln, D., Wefer, G., 1997. Late Quaternary palaeoceanography in the Fram Strait. Palaeoceanography 12, 65–78.

Hibler, W.D., 1989. Arctic ice-ocean dynamics. In: Herman, Y. (Ed.), The Arctic Seas, Climatology, Oceanography, Geology and Biology. Van Nostrand Reinhold, New York, pp. 47–91.

Hulth, S.T., Blackburn, H., Hall, P.O.J., 1994. Arctic sediments (Svalbard): consumption and microdistribution of oxygen. Mar. Chem. 46, 293–316.

Hulth, S.T., Hall, P.O.J., Blackburn, H., Landen, A., 1996. Arctic sediments (Svalbard): pore water and solid hase distributions of C, N and Si. Polar Biol. 16, 447–462.

Ishman, S.E., Foley, K.M., 1996. Modern benthic foraminifer distribution in the Amerasian Basin, Arctic Ocean. Micropalaeontology 42, 206–220.

Jansen, E., Erlenkeuser, H., 1985. Ocean circulation in the Norwegian Sea during the last deglaciation: isotopic evidence. Palaeogeogr. Palaeoclimatol. Palaeoecol. 49, 189–206.

Johnsen, S.J., Dahl-Jensen, D., Gundestrup, N., Steffensen, J.P., Clausen, H.B., Miller, H., Masson-Delmotte, V., Sveinbjörnsdottir, A.E., White, J., 2001. Oxygen isotope and palaeotemperature records from six Greenland ice-core stations: Camp Century, Dye-3, GRIP, GISP2, Renland and NorthGRIP. J. Quat. Sci. 16, 299–307.

Jones, G.A., Keigwin, L.D., 1988. Evidence from Fram Strait (78°N) for early deglaciation. Nature 336, 56–59.

Jongman, R.H.G., Ter Braak, C.J.F., Van Tongeren, O.F.R.,

1995. Data Analysis in Community and Landscape Ecology. Cambridge University Press, Cambridge.

Knies, J., Vogt, C., Stein, R., 1999. Growth and decay patterns of the Svalbard/Barents Sea ice-sheet and palaeoceanographic evolution during Saalian and Weichselian glaciations. Geo-Mar. Lett. 18, 195–202.

Knies, J., Müller, C., Nowaczyk, N., Stein, R., 2000. A multi-proxy approach to reconstruct the environmental changes along the Eurasian continental margin over the last 160,000 years. Mar. Geol. 163, 317–344.

Koblents-Mishke, O.I., Volkovinsky, V.V., Kabanova, J.G., 1968. Noviie dannie o velichine pervichnoi produktsii mirovogo okena. Dokl. Akad. Nauk. SSSR 183, 1189–1192.

Koblents-Mishke, O.I., Volkovinsky, V.V., Kabanova, J.G., 1970. Plankton primary production of the world ocean. In: Wooster, W. (Ed.), Scientific Exploration of the South Pacific. National Academy of Science, Washington, DC, pp. 183–193.

Kotlyakov, V.M., Liouty, A.A., Finko, E.A., Krenke, A.N., Leonov, Yu.G., Velichko, A.A., 1998. Resources and Environment World Atlas. Geographisches Institut Hölzel, Vienna.

Kröncke, I., Tan, T.L., Stein, R., 1994. High benthic bacteria standing stock in deep Arctic basins. Polar Biol. 14, 423–428.

Lambeck, K., 1995. Constraints on the Late Weichselian ice sheet over the Barents Sea from observations of raised shorelines. Quat. Sci. Rev. 14, 1–16.

Lampitt, R.S., Antia, A.N., 1997. Particle flux in deep seas: regional characteristics and temporal variability. Deep-Sea Res. 44, 1377–1403.

Landvik, J.Y., Bondebik, S., Elverhoi, A., Fjeldskaar, W., Mangerud, J., Siegert, S., Salvigsen, O., Svendsen, J.-I., Vorren, T.O., 1998. The Last Glacial Maximum of Svalbard and the Barents Sea Area: Ice-sheet extent and configuration. In: Rose, J. (Ed.), Glacial and Oceanic History of the Polar North Atlantic Margins. Quat. Sci. Rev. 17, 43–77.

Lara, R.J., Kattner, G., Tillmann, U., Hirche, H.-J., 1994. The North East Water Polynya (Greenland Sea). II. Mechanisms of nutrient supply and influence on phytoplankton distribution. Polar Biol. 14, 483–490.

Linke, P., Lutze, G.F., 1993. Microhabitat preferences of benthic foraminifera a static concept or a dynamic adaptation to optimize food acquisition? Mar. Micropaleontol. 20, 215–234.

Longhurst, A., Sathyendranath, S., Platt, T., Caverhill, C., 1995. An estimate of global primary production in the ocean from satellite radiometer data. J. Plankton Res. 17, 1245–1271.

Louanchi, F., Najjar, R.G., 2001. Annual cycles of nutrients and oxygen in the upper layers of the North Atlanic Ocean. Deep-Sea Res. II 48, 2155–2171.

Loubere, P., 1994. Quantitative estimation of surface ocean productivity and bottom water oxygen concentration using benthic foraminifera. Paleoceanography 9, 723–737.

Loubere, P., 2000. Marine control of biological production in the eastern equatorial Pacific Ocean. Nature 406, 497–500.

Loubere, P., Fariduddin, M., 1999. Quantitative estimation of global patterns of surface ocean biological productivity and its seasonal variation on timescales from centuries to millennia. Global Biogeochem. Cycles 13, 115–133.

Lubinski, D.J., Polyak, L., Forman, S.L., 2001. Freshwater and Atlantic Water inflows to the deep northern Barents and Kara seas since ca. 13 ^{14}C ka: Foraminifera and stable isotopes. Quat. Sci. Rev. 20, 1851–1879.

Mackensen, A., Hald, M., 1988. *Cassidulina teretis* Tappan and *C. laevigata* D'Orbigny. Their Modern and Late Quaternary distribution in northern seas. J. Foram. Res. 18, 16–24.

Mangerud, J., Jansen, E., Landvik, J.Y., 1996. Late Cenozoic history of the Scandinavian and Barents Sea ice-sheets. In: Solheim, A., Riis, F., Elverøi, A., Fleide, J.J., Jensen, L.N., Cloething, S. (Eds.), Impact of Glaciations on Basin Evolution: Data and Models from the Norwegian Margin and Adjacent Areas. Global Planet. Change 12, 11–26.

Mangerud, J., Dokken, T., Hebbeln, D., Heggen, B., Ingolfsson, O., Landvik, J.Y., Mejdahl, V., Svendsen, J.I., Vorren, T.O., 1998. Fluctuations of the Svalbard-Barents Sea ice-sheet during the last 150000 years. Quat. Sci. Rev. 17, 11–42.

Mangerud, J., Astakhov, V., Svendsen, J.-I., 2002. The extend of the Barents-Kara ice-sheet during the Last Glacial Maximum. Quat. Sci. Rev. 21, 111–119.

Martin, J.H., Knauer, G.A., Karl, D.M., Broenkow, W.W., 1987. VERTEX: carbon cycling in the northeast Pacific. Deep-Sea Res. 34, 267–285.

Matthiessen, J., Knies, J., Nowaczyk, N.R., Stein, R., 2001. Late Quaternary dinoflagellate cyst stratigraphy at the Eurasian continental margin, Arctic Ocean: Indications for Atlantic water inflow in the past 150,000 years. Global Planet. Change 31, 65–86.

Melnikov, I.A., 1997. The Arctic Sea Ice ecosystem. Gordon and Breach, Amsterdam.

Moore, T.C., Jr., Walker, J.C.G., Rea, D.K., Lewis, C.F.M., Shane, L.C.K., Smith, A.J., 2000. Younger Dryas interval and outflow from the Laurentide ice-sheet. Palaeoceanography 15, 4–18.

Murray, J.W., Alve, E., 1994. High diversity agglutinated foraminiferal assemblages from the NE Atlantic: Dissolution experiments. Cush. Found Spec. Publ. 32, 33–51.

Nees, S., 1997. High-resolution benthic foraminiferal records of the last glacial temination in the northern North Atlantic. In: Hass, H.C., Kaminski, M.A. (Eds.), Contribution to the Micropaleontology and Paleoceanography of the Northern North Atlantic. Grzybowski Found. Spec. Publ. 5, 167–197.

Nees, S., Struck, U., 1994. The biostratigraphic and palaeoceanographic significance of *Siphotextularia rolshauseni* Phleger and Parker in Norwegian-Greenland Sea sediments. J. Foram. Res. 24, 233–240.

Nees, S., Altenbach, A.V., Kassens, H., Thiede, J., 1997. High resolution record of foraminiferal response to late Quaternary sea-ice retreat in the Norwegian-Greenland Sea. Geology 25, 659–662.

Nørgaard-Pedersen, N., Spielhagen, R.F., Thiede, J., Kassens,

H., 1998. Central Arctic surface ocean environment during the past 80,000 years. Palaeoceanography 13, 193–204.

Nørgaard-Pedersen, N., Spielhagen, R.F., Erlenkeuser, H., Grootes, P.M., Heinemeier, J., Knies, J., 2003. The Arctic Ocean during the Last Glacial Maximum: atlantic and polar domains of surface water mass distribution and ice cover. Paleoceanography 18, 1–19.

Oppo, D.W., Lehman, S.J., 1995. Suborbital timescale variability of North Atlantic Deep Water during the past 200,000 years. Palaeoceanography 10, 901–910.

Osterman, L.E., Poore, R.Z., Foley, K.M., 1999. Distribution of benthic foraminifers (>125 μm) in the surface sediments of the Arctic Ocean. U.S. Geol. Surv. Bull. 2164.

Pace, M.L., Knauer, G.A., Karl, D.M., Martin, J.H., 1987. Primary production, new production and vertical flux in the eastern Pacific Ocean. Nature 325, 803–804.

Pagels, U., 1991. Sedimentologische Untersuchungen und Bestimmung der Karbonatlösung in spätquartären Sedimenten des östlichen Arktischen Ozeans. Geomar Report, 10, University of Kiel, Kiel.

Piepenburg, D., Chernova, N.V., v. Dorrien, C.F., Gutt, J., Neyelov, A.V., Rachor, E., Saldanha, L., Schmid, M.K., 1996. Megabenthic communities in the waters around Svalbard. Polar Biol. 16, 431–446.

Polyak, L.V., 1990. General trends of benthic foraminifera distribution in the Arctic Ocean. In: Kotlyakov, V.M., Sokolov, V.E. (Eds.), Arctic Research, Advances and Prospects, Part 2. Nauka, Moscow, pp. 211–212.

Polyak, L., Solheim, A., 1994. Late- and postglacial environments in the northern Barents Sea west of Franz Josef Land. Polar Res. 13, 197–207.

Polyak, L., Mikhailov, V., 1996. Post-glacial environments of the southeastern Barents Sea: foraminiferal evidence. In: Andrews, J.T., Austin, W.E.N., Bergsten, H., Jennings, A.E. (Eds.), Late Quaternary Palaeoceanography of the North Atlantic Margins. Geol. Soc. Spec. Publ. III, 323–339.

Pomeroy, L.R., 1997. Primary production in the Arctic Ocean estimated from dissolved oxygen. J. Mar. Syst. 10, 1–8.

Poore, P.Z., Osterman, L., Curry, W.B., Philips, R.L., 1999. Late Pleistocene and Holocene meltwater events in the western Arctic Ocean. Geology 27, 750–762.

Rachor, E., 1992. Scientific Report of RV 'Polarstern' Cruise ARK-VIII/2. Ber. Polarforsch. 115.

Rahmstorf, S., 1995. Bifurcations of the Atlantic thermohaline circulation in response to changes in the hydrological cycle. Nature 378, 145–149.

Rasmussen, T.L., Thomsen, E., van Weering, T.C.E., Labeyrie, L., 1996. Rapid changes in surface and deep water conditions at the Faeroe Margin during the last 58,000 years. Paleoceanography 11, 757–771.

Reimnitz, E., Graves, S.M., Barnes, P.W., 1988. Beaufort Sea coastal erosion, sediment flux, shoreline evolution, and the erosional shelf profile. U.S. Geological Survey, to accompany Map I-1182-G, 22 pp.

Rochon, A., de Vernal, A., Turon, J.-L., Matthiessen, J., Head, M.J., 1999. Distribution of dinoflagellate cysts in surface sediments from the North Atlantic Ocean and adjacent basins and quantitative reconstruction of sea-surface parameters. Am. Assoc. Stratigr. Palynol. Contr. Ser. 35, 150 pp.

Rudels, B., Jones, E.P., Anderson, L.G., Kattner, G., 1994. On the intermediate depth water of the Arctic Ocean. In: Johannessen, O.M., Muench, R.D., Overland, J.E. (Eds.), The Polar Oceans and Their Role in Shaping the Global Environment – The Nansen Centennial Volume. Geophys. Monogr. Ser. 85, 33–46.

Rudels, B., Meyer, R., Fahrbach, E., Ivanov, V.V., Østerhus, S., Quadfasel, D., Schauer, U., Tverberg, V., Woodgate, R.A., 2000. Water mass distribution in Fram Strait and over the Yermak Plateau in summer 1997. Ann. Geophys. 18, 687–705.

Sarnthein, M., Pflaumann, U., Ross, R., Tiedemann, R., Winn, K., 1992. Transfer-functions to reconstruct ocean palaeoproductivity: a comparison. In: Summerhays, C.P., Prell, W.L., Emeis, K.C. (Eds.), Upwelling Systems: Evolution since the Early Miocene. Geol. Soc. Spec. Publ. 64, 411–427.

Sarnthein, M., Stattegger, K., Dreger, D., Erlenkeuser, H., Grootes, P., Haupt, B., Jung, S., Kiefer, T., Kuhnt, W., Pflaumann, U., Schäfer-Neth, C., Schulz, H., Schulz, M., Seidov, D., Simstich, J., van Krefeld-Alfane, S., Vogelsang, E., Völker, A., Weinelt, M., 2000. Fundamental modes and abrupt changes in North Atlantic circulation and climate over the last 60 ky – Numerical modelling and reconstruction. In: Schäfer, P., Ritzrau, W., Schlüter, M., Thiede, J. (Eds.), The Northern North Atlantic: A Changing Environment. Springer-Verlag, Berlin, pp. 365–410.

Schlichtholz, P., Houssais, M.-N., 1999. An inverse modeling study in Fram Strait. Part I: dynamics and circulation. Deep-Sea Res. II 46, 1083–1135.

Schlüter, M., Sauter, E.J., Schäfer, A., Ritzrau, W., 2000. Spatial budget of organic carbon flux to the seafloor of the northern North Atlantic (60°N–80°N). Global Biogeochem. Cycles 14, 329–340.

Schubert, C.J., Stein, R., 1996. Deposition of organic carbon in Arctic Ocean sediments: terrigenous supply vs marine productivity. Org. Geochem. 24, 421–436.

Scott, D.B., Mudie, P.J., Baki, V., MacKinnon, K.D., Cole, F.E., 1989. Biostratigraphy and late Cenozoic paleoceanography of the Arctic Ocean. Foraminifera, lithostratigraphic, and isotopic evidence. Geol. Soc. Am. Bull. 101, 260–277.

Scott, D.B., Vilks, G., 1991. Benthonic foraminifera in the surface sediments of the deep-sea Arctic Ocean. J. Foram. Res. 21, 20–38.

Sejrup, H.P., Jansen, E., Erlenkeuser, H., Holtedahl, H., 1984. New faunal and isotopic evidence on the Late Weichselian-Holocene oceanographic changes in the Norwegian Sea. Quat. Res. 21, 74–84.

Smart, C.W., King, S.C., Gooday, A.J., Murray, J.W., Thomas, E., 1994. A benthic foraminiferal proxy of pulsed organic matter palaeofluxes. Mar. Micropaleontol. 23, 89–99.

Smith, W.O., Baumann, M.E.M., Wilson, D.L., Aletsee, L., 1987. Phytoplankton biomass and productivity in the mar-

ginal ice zone of the Fram Strait during summer 1984. J. Geophys. Res. 92, 6777–6786.

Smith, W.O., Jr., Walsh, I.D., Booth, B.C., Deming, J.W., 1995. Particulate matter and phytoplankton and bacterial biomass distributions in the Northeast Water Polynya during summer 1992. J. Geophys. Res. 100, 4357–4370.

Smith, W.O., Jr., Gosselin, M., Legendre, L., Wallace, D.W.R., Daly, K.L., Kattner, G., 1997. New production in the Northeast Water Polynya: 1993. J. Mar. Syst. 10, 199–209.

Springer, A.M., McRoy, C.P., 1993. The paradox of pelagic food webs in the northern Bering Sea – III. Patterns of primary production. Cont. Shelf Res. 13, 575–599.

Stein, R., Nam, S.-I., Schubert, C., Vogt, C., Fütterer, D.K., Heinemeier, J., 1994. The last deglaciation event in the eastern central Arctic Ocean. Science 264, 692–696.

Stein, R., Fahl, K., 1997. Scientific Cruise Report of the Arctic Expedition ARK-XIII/2 of RV 'Polarstern' in 1997. Ber. Polarforsch. 255.

Stein, R., Fahl, K., Niessen, F., Siebold, M., 1999. Late Quaternary organic carbon and biomarker records from the Laptev Sea continental margin (Arctic Ocean): Implications for organic carbon flux and composition. In: Kassens, H., Bauch, H.A., Dmitrenko, I.A., Eicken, H., Hubberten, H.-W., Melles, M., Thiede, J., Timokhov, L.A. (Eds.), Land-Ocean Systems in the Siberian Arctic: Dynamics and History. Springer-Verlag, Berlin, pp. 635–655.

Stein, R., Fahl, K., 2000. Holocene accumulation of organic carbon at the Laptev Sea continental margin (Arctic Ocean): sources, pathways, and sinks. Geo-Mar. Lett. 20, 27–36.

Steinsund, P.I., Hald, M., 1994. Recent calcium carbonate dissolution in the Barents Sea, Palaeoceanographic applications. Mar. Geol. 117, 303–316.

Stötter, J., Wastl, M., Caseldine, C., Häberle, T., 1999. Holocene palaeoclimatic reconstruction in northern Iceland: approaches and results. Quat. Sci. Rev. 18, 457–474.

Strömberg, J.O., 1989. Northern Svalbard waters. In: Rey, L., Rey, V. (Eds.), Proceedings of the Sixth Conference Comité Arctique International, Leiden, pp. 402–426.

Struck, U., 1997. Paleoecology of benthic foraminifera in the Norwegian-Greenland Sea during the past 500 ka. In: Hass, H.C., Kaminski, M.A. (Eds.), Contribution to the Micropaleontology and Paleoceanography of the Northern North Atlantic. Grzybowski Found. Spec. Publ. 5, 51–82.

Stuiver, M., Reimer, P.J., 1993. Extended 14C database and revised CALIB radiocarbon calibration program. Radiocarbon 35, 215–230.

Stuiver, M., Reimer, P.J., Bard, E., Beck, J.W., Burr, G.S., Hughen, K.A., Kromer, B., McCormac, G., van der Plicht, J., Spurk, M., 1998. INTCAL 98 radiocarbon age calibration, 24,000–0 cal BP. Radiocarbon 40, 1041–1083.

Suess, E., 1980. Particulate organic carbon flux in the oceans: Surface productivity and oxygen utilization. Nature 288, 260–263.

Svendsen, J.I., Astakov, V.I., Bolshiyanov, D.Y., Demidov, I., Dowdeswell, J.A., Gataullin, V., Hjort, C., Hubberten,

H.W., Larsen, E., Mangerud, J., Melles, M., Möller, P., Saarnisto, M., Siegert, M.J., 1999. Maximum extent of the Eurasian ice-sheets in the Barents and Kara Sea region during the Weichselian. Boreas 28, 234–242.

ter Braak, C.J.F., Smilauer, P., 1998. CANOCO Reference Manual and User's Guide to Canoco for Windows: Software for Canonical Community Ordination (version 4). Microcomputer Power, Ithaca, NY.

Thomas, E., Booth, L., Maslin, M., Shackleton, N.J., 1995. Northeastern Atlantic benthic foraminifera during the last 45,000 years: Changes in productivity seen from the bottom up. Paleoceanography 10, 545–562.

van Andel, T.H., Hearth, G.R., Moore, T.C., 1975. Cenozoic history and palaeoceanography of the Central Equatorial Pacific. Mem. Geol. Soc. Am. 143, 1–134.

Vézina, A.F., Savenkoff, C., Roy, S., Klein, B., Rivkin, R., Therriault, J.-C., Legendre, L., 2000. Export of biogenic carbon and structure and dynamics of the pelagic food web in the Gulf of St. Lawrence. Part 2. Inverse analysis. Deep-Sea Res. II 47, 609–635.

Vilks, G., 1969. Recent foraminifera in the Canadian Arctic. Micropaleontology 15, 35–60.

Vilks, G., 1989. Ecology of Recent foraminifera on the Canadian Continental Shelf of the Arctic Ocean. In: Herman, Y. (Ed.), The Arctic Seas, Climatology, Oceanography, Geology and Biology. Van Nostrand Reinhold, New York, pp. 497–569.

Vogelsang, E., 1990. Paläo-Ozeanographie des Europäischen Nordmeeres an Hand stabiler Kohlenstoff- und Sauerstoffisotope. Ph.D. Thesis, Ber. Sonderforschungsberichte 313, 23, Univsity of Kiel, Kiel.

Vorren, T.O., Laberg, J.S., 1996. Late glacial air temperature, oceanographic and ice-sheet interactions in the southern Barents Sea region. In: Andrews, J.T., Austin, W.E.N., Bergsten, H., Jennings, A.E. (Eds.), Late Quaternary Palaeoceanography of the North Atlantic Margins. Geol. Soc. Spec. Publ. III, 303–322.

Wassman, P., Slagstad, D., 1991. Annual dynamics of carbon flux in the Barents Sea. Preliminary results. Norsk Geol. Tidsskr. 71, 231–234.

Weinelt, M., Kuhnt, W., Sarnthein, M., Altenbach, A., Costello, O., Erlenkeuser, H., Pflaumann, U., Simstich, J., Struck, U., Thies, A., Trauth, M.H., Vogelsang, E., 2000. Paleoceanographic proxies in the northern North Atlantic. In: Schäfer, P., Ritzrau, W., Schlüter, M., Thiede, J. (Eds.), The Northern North Atlantic: A Changing Environment. Springer-Verlag, Berlin, pp. 319–352.

Wefer, G., 1993. Formation and composition of marine particulates. In: Heimann, M. (Ed.), The global carbon cycle. Nato ASI Series 115, 505–530.

Wheeler, P.A., Gosselin, M., Sherr, E., Thibault, D., Kirchman, D.L., Benner, R., Whitledge, T.E., 1996. Active cycling of organic carbon in the central Arctic Ocean. Nature 380, 697–699.

Wollenburg, J.E., Mackensen, A., 1998a. Modern benthic foraminifers from the central Arctic Ocean. Mar. Micropaleontol. 34, 153–185.

Wollenburg, J.E., Kuhnt, W., 2000. The response of benthic foraminifers to carbon flux and primary production in the Arctic Ocean. Mar. Micropaleontol. 40, 189–231.

Wollenburg, J.E., Kuhnt, W., Mackensen, A., 2001. Changes in Arctic Ocean palaeoproductivity and hydrography during the last 145 kyr: the benthic foraminiferal record. Paleoceanography 16, 65–77.

Zheng, Y., Schlosser, P., Swift, J.H., Jones, E.P., 1998. Oxygen utilization rates in the Nansen Basin, Arctic Ocean: implications for new production. Deep-Sea Res. 44, 1923–1943.